

# **RECRYSTALLIZATION TEXTURE DEVELOPMENT IN CP- TITANIUM**

A THESIS SUBMITTED IN PARTIAL FULLFILLMENT OF THE  
REQUIREMENT FOR THE DEGREE OF

**Masters of Technology**

**In**

Metallurgical and Materials Engineering

**By**

**BAIDEHISH SAHOO (211MM1367)**



**DEPARTMENT OF METALLURGICAL AND MATERIALS  
ENGINEERING NATIONAL INSTITUTE OF  
TECHNOLOGY, ROURKELA**

**May, 2013**

# **RECRYSTALLIZATION TEXTURE DEVELOPMENT IN CP- TITANIUM**

A THESIS SUBMITTED IN PARTIAL FULLFILLMENT OF THE  
REQUIREMENT FOR THE DEGREE OF

**Masters of Technology**

**In**

Metallurgical and Materials Engineering

By

**BAIDEHISH SAHOO (211MM1367)**

UNDER THE GUIDANCE

OF

**PROF. SANTOSH KUMAR SAHOO**



**DEPARTMENT OF METALLURGICAL AND MATERIALS  
ENGINEERING NATIONAL INSTITUTE OF  
TECHNOLOGY, ROURKELA**

**May, 2013**



**National Institute of Technology**

**CERTIFICATE**

This is to certify that the thesis entitled “**Recrystallization Texture development in CP-Titanium**” being submitted by **Baidehish Sahoo (211MM1367)** for the partial fulfillment of the requirements of Masters of Technology degree in Metallurgical and Materials engineering is a bonafide thesis work done by him under my supervision during the academic year 2012-2013, in the Department of Metallurgical and Materials Engineering, National Institute of Technology Rourkela, India.

The results presented in this thesis have not been submitted elsewhere for the award of any other degree or diploma.

Date:

**(Prof. Santosh Kumar Sahoo)**  
Metallurgical and Materials  
Engineering  
National Institute of Technology  
Rourkela  
Rourkela, Odisha- 769008



## ACKNOWLEDGMENT

---

We take this opportunity to express our deepest regards and sincere gratitude to our guide **Prof. Santosh Kumar Sahoo** for his constant guidance and concern throughout the project. He will always remain a constant source of inspiration for us. We also express our sincere gratitude to **Dr. B.C. Ray, HOD**, Metallurgical and Materials Engineering for providing valuable departmental facilities. We are very thankful to **Prof. Indradev Samajdar** of **IIT Bombay**, for his constant support in conducting experiments. We extend our thanks to **Prof. Satyam Suwas, IISC Bangalore**, who has helped us with accumulative roll bonding of samples during the project. We are also thankful to technical assistants of Department of Metallurgical and Materials Engineering, NIT Rourkela, for their constant practical assistance and help whenever required. We would also like to thank all the staff members of Metallurgical and Materials Engineering department and everyone who in some way or the other has provided us valuable guidance, suggestion and help in this project.

Place: NIT Rourkela  
Date:

Baidehish Sahoo (211MM1367)

## ABSTRACT

---

Understanding of recrystallization texture, the objective of the present study, is very important because most of the engineering components subjected to annealing as a final forming operation before different applications. Such recrystallization texture is well established in cubic materials compared to hexagonal materials. In the present study recrystallization texture development in CP-titanium was investigated. CP-titanium grade-2 plates were subjected to cold rolling of 90% reduction in thickness. The rolled plates were annealed at 700°C for 5hrs. Such annealed plates were then subjected to accumulative roll bonding (ARB) for 6 passes. The ARB processed samples were then subjected to isochronal annealing at 200°C, 300°C, 400°C, 500°C and 600°C for 1hr to obtain the recrystallization temperature. Final annealing of the ARB processed samples was carried out at 600°C for different soaking time: 5sec, 10sec, 20sec, 30sec, 60sec, 120sec, 300sec, 600sec, 1200sec, 1800sec and 3600sec, to establish the texture development during annealing. The annealed samples were subsequently characterized under XRD (X-ray Diffraction) for bulk texture measurement and EBSD (Electron backscattered diffraction) for micro-texture and microstructural developments. Strengthening of (11-24)<31-4-1> orientation with increasing annealing time was observed.

**Keywords:** *Recrystallization texture, CP-titanium, hexagonal metals, ARB*

# **CONTENT**

Certificate	i
Acknowledgements	ii
Abstract	iii
List of Figures	iv
List of Tables	v
<b>CHAPTER 1 INTRODUCTION</b>	
1.0 Introduction	1
1.2 Objectives	2
<b>CHAPTER 2 LITERATURE REVIEW</b>	
2.1 Introduction	3
2.2 Texture Representation	5
2.2.1 Pole Figure	5
2.2.2 Orientation Distribution Function (ODF)	6
2.2.2.1 Euler Angles	6
2.2.2.2 Euler Space	8
2.3 Recrystallization Texture	8
2.3.1 Recrystallization Texture in HCP Metals	11
2.4 Recrystallization Textures in CP Titanium	12
2.5 Accumulative Roll Bonding (ARB)	12
<b>CHAPTER 3 EXPERIMENTS</b>	
3.1 Material and Sample Preparation	15
3.2 Characterization Techniques	16
3.2.1 X-Ray Diffraction (XRD)	16
3.2.2 Electron Backscattered Diffraction (EBSD)	16
<b>CHAPTER 4 RESULTS AND DISCUSSION</b>	
4.1 Recrystallization Temperature	17
4.2 Texture Determination	35

## **CHAPTER 5**

Conclusion	32
Scope for further study	32
Reference	33

## **List of Figures**

Fig. 2.1	a) Grains are crystallographically similarly arranged, b) grains are crystallographically differently arranged, and c) some grains are crystallographically similarly and some are differently arranged. .	3
Fig. 2.2	Schematic showing construction of a (100) pole figure	6
Fig. 2.3	Orientation of the crystal axis system ( $X_i^\circ$ ) and the sample axis system {RD, TD, ND}; $s$ is the intersection of the planes (RD–TD) and ([100]–[010]).	7
Fig. 2.4	Definition of Euler angles, $\phi_1$ , $\Phi$ and $\phi_2$ , in Bunge convention	7
Fig. 2.5	Representation of Euler space with Euler angles.	8
Fig. 2.6	Schematics of accumulative roll bonding	13
Fig. 4.1	Image quality (IQ) maps of isochronal annealing (for 1hr) of cp-titanium samples at 500°C (a) and 600°C (b).	18
Fig. 4.2	Inverse pole figure (IPF) maps of isochronal annealing (for 1hr) of cp-titanium samples at 500°C (a) and 600°C (b).	18
Fig. 4.3	Image quality (IQ) maps of cp-titanium annealed at 600°C for; (a) 600sec, (b) 1200sec, (c) 1800sec, and (d) 3600sec.	19
Fig. 4.4	Percentage of recrystallization as a function of annealing time during annealing of cp-titanium at 600°C.	19
Fig.4.5	XRD plot of cp-titanium samples annealed at 600°C for different soaking time	20
Fig.4.6	ODF plots, at constant $\phi_2$ , of different annealed cp-titanium samples. The contour levels are similar in all the plots.	29
Fig.4.7	Maximum ODF intensity (maximum $f(g)$ ) values as a function of annealing time for the annealed cp-titanium samples.	29



## **LIST OF TABLES**

Table.3.1	Chemical composition (in wt.%) of CP titanium used in the Present study	16
Table 4.1	Pole figures of different annealed cp-titanium samples.	20
Table 4.2	Important texture developments during annealing of cp-titanium	30

### 1.0 Introduction

Over few decades the researchers are mostly involved in establishing texture development for different properties of a material. It has been well understood that texture of a material is dependent on plastic deformation [1,2] and/or phase transformation [3]. Recrystallization texture is a type of (phase transformation) texture developed during annealing of a material. Study of this texture is very important because annealing is the final processing step for fabrication of any engineering component.

Recrystallization texture development in cubic metals is widely studied in the literature [4-7]. Also the mechanism of such texture development in cubic metals is well established by the researchers [8-10], as compared to hexagonal metals. There are two competing recrystallization theories, which give idea about recrystallization texture: oriented nucleation theory (ON) and oriented growth theory (OG) [11, 12]. It is assumed that in a deformed matrix some grains or zones have more potent nuclei than others. This suggestion is based on the observation that certain sites are preferred sites for nucleation of recrystallized grains, for example: persistent cube bands, zone around non shearable second phase, shear bands, etc [13]. In other words some kind of preferred nucleation exists in the deformed matrix and is called oriented nucleation. As per oriented growth theory, all potential nuclei are activated without any preference. But those nuclei which have a fast growing grain boundary in nature compared to their neighbour will develop much faster and will determine the recrystallization texture.

Although in hexagonal metals the recrystallization texture development is not well known, some studies have been reported on texture development during annealing of hexagonal metals [14-16]. In the present study the recrystallization texture development in commercial purity (cp) titanium is investigated. For such understanding the cp-titanium was subjected to accumulative roll bonding (ARB) to achieve ultrafine grains, and subsequently it is annealed. The annealing was carried out at the recrystallization temperature (600°C) for a very small soaking time to a larger soaking time.

## **1.1 OBJECTIVE**

- A systematic characterization of texture development during annealing of ARB processed cp-titanium.
- Understanding the important recrystallization texture developments in cp-titanium.
- Comparison of recrystallization texture development with cold rolled & annealed cp-titanium.

#### 2.1 Introduction

It has been quoted that the influence of texture on material properties is, in many cases, 20-50% of the property values [17]. The word texture derived from the Latin word ‘textor’ which means weaver [18]. In material science, texture of a material means how a material is woven. In simple words texture means how the individual constituent or the building blocks of a material are arranged [19]. There are three possible cases for a polycrystalline material where, (a) the individual grains are crystallographically similarly arranged, (b) the individual grains are differently arranged or (c) some of the grains are crystallographically similarly arranged and some are differently arranged. In this way the materials are respectively termed as textured, randomized or partially textured materials. Such three conditions of a material are shown in figure 2.1.

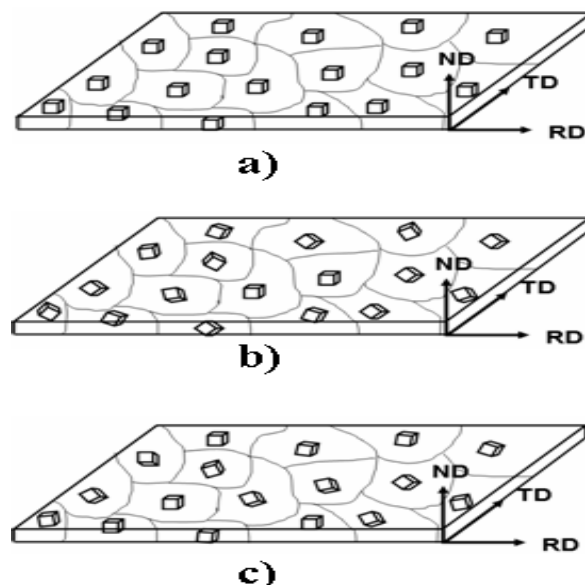


Figure 2.1. a) Grains are crystallographically similarly arranged, b) grains are crystallographically differently arranged, and c) some grains are crystallographically similarly and some are differently arranged.

If we consider the first case then it is the result of a single crystal while the other two cases refer to a polycrystalline material with random/partially textured orientation [17, 19]. The preferred orientation or texture is mainly divided into two types such as: (i) deformation

texture and (ii) annealing/recrystallization texture [18]. The texture development during plastic deformation is known as deformation texture and that during annealing is known as annealing/recrystallization texture [13, 18]. However, the texture may also change during casting, welding etc. In case of a polycrystalline material the material properties depends upon the individual grain morphology and orientation. When all possible crystallographic orientation occur in a polycrystalline material with same frequencies, then the properties that depends upon the crystallographic orientation cancels out due to averaging and the material can be said as a isotropic material on an average. But for all application we don't need a material with isotropic properties. For example in case of deep drawing operation semi-isotropic property of the material is needed to avoid earing [17, 20, 21]. Another example is pressure vessel. In case of a pressure vessel the stresses experienced by vessel in longitudinal direction is twice that of the circumferential direction [17]. So to avoid failure of the vessel material with anisotropic properties is preferred. For different engineering application we need materials with specific properties. If the individual grains are nearly similarly oriented then the polycrystalline material behaves like single crystal. 'Cube' texture in case of a body centred cubic (BCC) material or face centred cubic (FCC) material is a very good example of this [22]. In this case all the grains are oriented in such a way that  $\{0\ 0\ 1\}$  plane lies almost parallel to the sheet plane and  $\langle 1\ 0\ 0 \rangle$  direction indicating the rolling direction. The texture  $\{0\ 0\ 1\} \langle 1\ 0\ 0 \rangle$  is highly desired in case of high temperature superconductor [23-25]. Like cube texture another texture is there known as Goss texture  $\{1\ 1\ 0\} \langle 0\ 0\ 1 \rangle$  [26,27]. The Goss texture is highly desirable in case of magnetic material in which it is easy to magnetize the material in the cube edge  $\langle 1\ 0\ 0 \rangle$ . Crystallographic texture is an intrinsic characteristic of metals, ceramics and geological materials. Mechanical, chemical as well as physical properties of a material are significantly influenced by crystallographic texture of that material [28-30]. The properties influenced by texture are modules of elasticity, strength, ductility, electrical conductivity, light refraction etc [31-32].

The objective of the present study was to investigate the recrystallization texture development during annealing of cp-titanium. In this chapter, the following sections will be reviewed in detail:

- Representation of texture (pole figure and orientation distribution function).
- Recrystallization texture.
- Recrystallization texture in titanium alloys.
- Accumulative roll bonding.

- Texture development during accumulative roll bonding.

## 2.2 Representation of Texture

The orientation of grains in a material is represented with respect to some external frame of reference. For flat products like sheets or plates this frame of reference consists of rolling direction (RD), a normal direction (ND) and transverse direction (TD). The texture or the preferred orientation is commonly represented by  $\{h\ k\ l\}$   $[u\ v\ w]$ . This represents the  $\{h\ k\ l\}$  plane is parallel to the sheet plane and the direction  $[u\ v\ w]$  is parallel to rolling direction [33, 34]. Pole figure and orientation distribution function are the two important methods for characterizing texture of a material.

### 2.2.1 Pole Figure

The pole figure is the most frequently used method of representing conventional textures. A pole figure is a 2-dimensional representation of a particular set of equivalent crystal orientations, following the principle of stereographic projection [17,18]. A schematic of (100) pole figure is represented in figure 2.2. In figure 2.2a, the Stereographic projection of (100) poles is represented and the projection of (100) poles of one grain on the equatorial plane is represented in 2.2b. Projection of the (100) poles of a polycrystal where the grains are randomly oriented is represented in 2.2c. Figure 2.2d shows the projection of (100) poles of a textured polycrystal, and this is usually represented as contour maps – as shown in figure 2.2e.

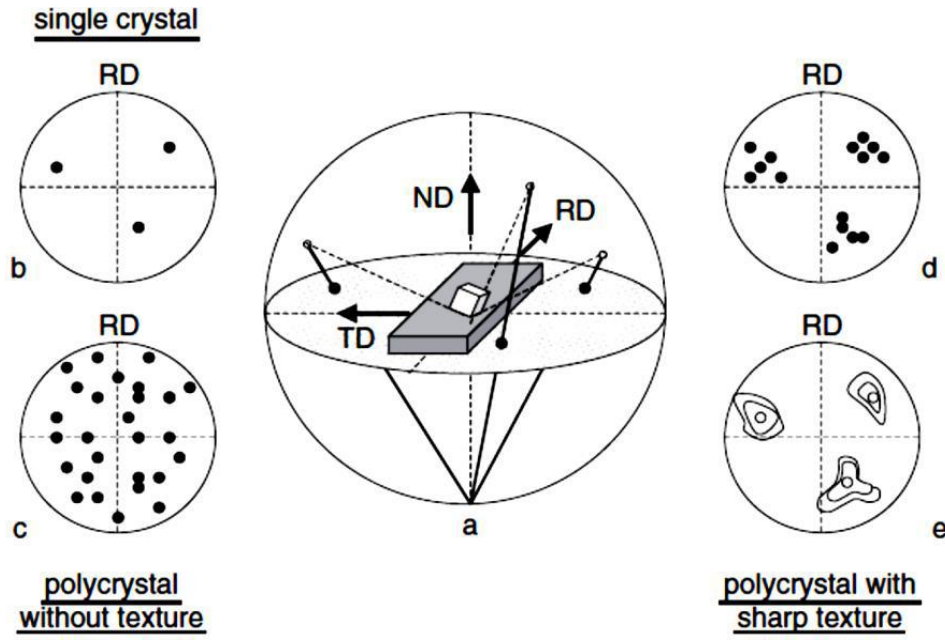


Figure 2.2. Schematic showing construction of a (100) pole figure [35].

### 2.2.2 Orientation Distribution Function (ODF)

There are certain limitations in pole figure representation of texture – in pole figure representation, it is necessary to analyze all intensities separately, and during projection it is always possible to miss certain orientations [17, 18, 36]. However, ODF describes complete texture information in a sample. An ODF is mathematically expressed as:

$$\frac{dV}{V} = f(g)dg$$

Where,  $g$  is the orientation of a grain and  $f$  is the volume fraction of grains in all intervals  $g \pm \Delta g$ . The ODF of a sample without texture is a constant. If the sample has a texture, the ODF has maxima and minima [36, 37].

#### 2.2.2.1 Euler Angles

Euler angles are used to define the orientation  $g$  of a grain, in order to give a graphical representation of an ODF. Two different co-ordinate systems are defined: the first is connected to the sample (sample axes system  $X_i$ ) and the second to the crystal of a grain (crystal axes system  $X_i^c$ ) – see figure 2.3. The sample system is related to the shape of the sample. For example, for a rolled sheet, the axis  $X_1$  is taken in the RD,  $X_2$  in the transverse and  $X_3$  in the ND of the sheet. The orientation of the crystal axes system can now be expressed in the reference frame of the sample axes system by three rotations (figure 2.4).

Though there are several conventions of performing these rotations, most widely used system is the system of Bunge.

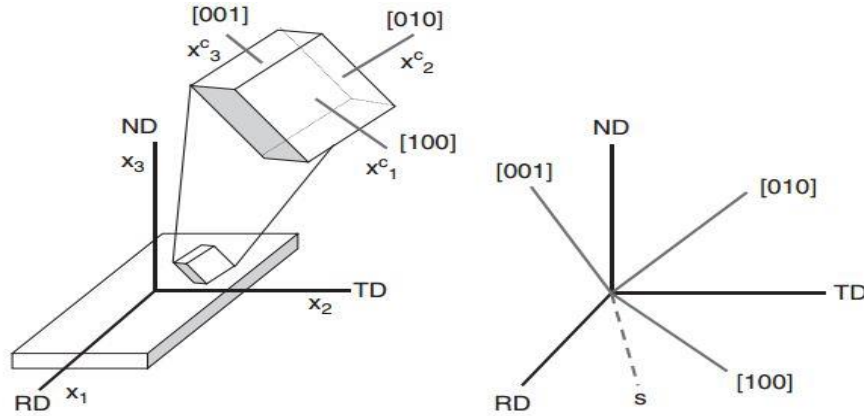


Figure 2.3. Orientation of the crystal axis system ( $X_i^c$ ) and the sample axis system {RD, TD, ND};  $s$  is the intersection of the planes (RD–TD) and ([100]–[010]). [38]

In Bunge system, first a,  $\phi_1$  rotation is performed around normal direction (ND) which brings RD in the position  $s$ , with  $s$  the intersection of the planes (RD–TD) and ([1 0 0] – [0 1 0]). Now the RD' and TD' are the new positions of RD and TD due to the rotation. Then a rotation around RD' by  $\Phi$  brings ND together with [0 0 1]. Because of this rotation position of TD' changes to TD". Finally a rotation of  $\phi_2$  around ND axis or about [0 0 1] is given. Due to this rotation RD' falls on [1 0 0] and TD" falls on [0 1 0]. The three angles ( $\phi_1$ ,  $\Phi$ ,  $\phi_2$ ) used for rotation about the different axes are called the Euler angles.

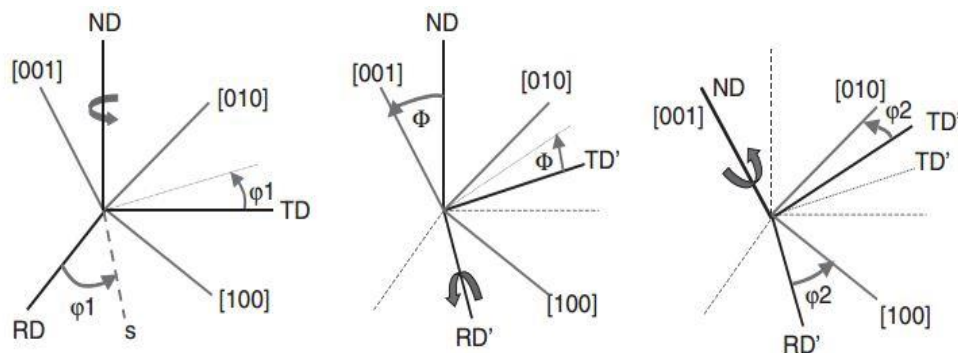


Figure 2.4. Definition of Euler angles,  $\phi_1$ ,  $\Phi$  and  $\phi_2$ , in Bunge convention. [39]



### 2.2.2.2 Euler Space

This is obtained by plotting the three Euler angles in Cartesian co-ordinates (figure 2.5). The angles  $\phi_1$  and  $\phi_2$  can be varied between  $0^\circ$  and  $360^\circ$  but the angle  $\Phi$  is varied between  $0^\circ$  and  $180^\circ$ . In this representation, individual orientations will be found at several locations.

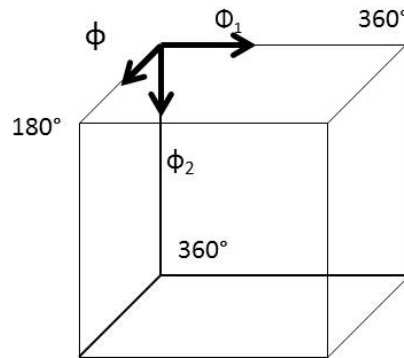


Figure 2.5. Representation of Euler space with Euler angles.

## 2.3 Recrystallization Texture

Recrystallization and phase transformation possess several common characteristics with the intention of replacement of deformed materials by nucleation and growth of new grains. Both can develop extreme changes in texture of the material. The major differences are (i) the “nuclei” during recrystallization are regions that previously exist in the deformed microstructure; and (ii) recrystallization does not direct to exact orientation relationship between the deformed and recrystallized materials unlike the case of phase transformation [4-8]. Even though there might be some estimated orientation relationships present between the recrystallized and parent grains [13] there has been no report in making quantitative predictions for recrystallization texture based on such approximate orientation relationships. The deformation structures developed during thermo-mechanical processing (TMP) are fundamentally unstable so that on annealing, after deformation processing, substructure evolution often occurs by thermally activated processes and this leads to a reduction of stored energy. These processes usually induce a substantial softening of the plastically deformed material. When a cold deformed material is annealed then the texture during the cold deformation is removed and a new texture evolves in the material. This new texture in the material is known as recrystallization texture. It is also known as ‘annealing texture’. The term ‘annealing texture’ is more appropriate in most of the practical situation as in most industrial annealing processes, a certain amount of grain growth cannot be barred or is in some cases even necessary. Since many industrial materials will receive their final forming

operation in annealed state, the understanding of recrystallization or annealing textures is very imperative. This texture to a large extent decides the material mechanical properties and also accountable for the mechanical anisotropy in the material. There is no general accepted mechanism of texture formation during annealing exists. The mechanism of recrystallization is not yet in every respect understood but it seems that small zones in the deformed matrix form the nuclei of the recrystallized grains [6,13,18]. This shows that the nucleus of a recrystallized grain will often have a similar orientation as the deformed region where it originates. But during deformation since grains can ‘break up’ into regions with small misorientations, the recrystallized grains will not have exactly same orientation as the grain we start with or the ‘mother grain’ [6,40]. The recrystallization texture would just be an imitation of the deformed texture if all grains would produce the same amount of nuclei and all nuclei would grow in the same manner, this is not a practical case. As the recrystallization texture is not same as the deformation texture so there must be some mechanism. The possibilities for this case: either some mother grains produce more potent nuclei than others, or some nuclei grow faster than others [40-42]. These two possibilities have given rise two competing recrystallization theories (i) the ‘oriented nucleation’ theory and (ii) the ‘oriented growth’ theory. According to oriented nucleation theory, it is proposed that in a deformed matrix some grains or zones have ‘more potent’ nuclei than others. This idea is based on the observation that certain sites are preferred sites for nucleation of recrystallized grains due to the difference in energy between the potential nucleus and it’s neighbouring [43,44], for example, persistent cube bands, zones around non-shearable 2nd phase particles, shear bands, etc. It is also experiential that in most of these favoured sites a prevalence of recrystallized grains with a meticulous orientation can be found, for example Goss  $\{0\ 1\ 1\} \langle 1\ 0\ 0 \rangle$  oriented grains in transition bands and in shear bands in steel or Cube  $\{100\} \langle 001 \rangle$  oriented grains in determined cube bands, S  $\{1\ 2\ 3\} \langle 6\ 3\ -4 \rangle$  grains in shear bands and randomly oriented grains around particles in aluminium alloys, etc []. Shear bands wounding across several grains may also act as a starting place of recrystallized grains. The formation of shear bands is often orientation sensitive [45,46]. Recrystallization is favoured from particle-deformed zones due to large differences in the stored energies. Recrystallization of this type is referred as particle stimulated nucleation (PSN) [47]. The particle-deformed zones, and correspondingly the PSN grains, are of randomized orientations. In particle-containing commercial alloys, the annealing behaviour, including recrystallization texture developments, is strongly influenced by annealing temperature. Low-temperature annealing is frequently related to stronger randomization [48]. To elucidate such behaviour, two approaches have been projected. The

first approach assumes the presence of inner and outer deformed zones – the former being more randomized [49]. An approach proposes that the relative assistance from PSN and deformation bands are accountable for the overall recrystallization behaviour, together with recrystallization texture developments [48]. Recrystallization twins are also accountable to play an important role in finding out the orientations of the recrystallized grains more valid for lower-SFE metals and alloys like copper, austenitic stainless steel. This is not a correct recrystallization mechanism but this is the barely mechanism which may outline recrystallized grains with new orientations [50]. The potency is often related to high stored energy and correspondingly large variations in relative misorientations and the possible presence of growth-favourable boundaries. From such interpretation it has been concluded that not all prospective nuclei (all orientations present in the deformed matrix) are really ‘activated’, but that some kind of preferred nucleation exist: oriented nucleation. According to oriented growth theory it is assumed that all potential nuclei are activated, without any predilection. But those nuclei which have a ‘fast growing’ grain boundary character with their neighbours will develop much faster and will conclude the recrystallization texture. This theory is based on the study that the components of a recrystallization texture can often be deduced from the deformation texture, by some scrupulous rotations around some simple crystal orientations. Some familiar examples are:

30–40° rotation around a common [1 1 1] axis in fcc metals.

25–30° rotation around a common [1 10] axis in bcc metals.

30° rotations around a common [0 0 0 1] axis or 90° around [1010] axis or 90° around [1 0 -1 0] in hexagonal metals.

An alternative is to describe the developments in recrystallized microstructure, in particular recrystallization texture, in terms of frequency and size advantage of recrystallized grains of different orientations [51]. During recrystallization suppose volume fraction of a particular component ‘*i*’ increases, then the increase in the volume due to more number of ‘*i*’ recrystallized grain or their greater sizes.

$$\alpha = \frac{i_{rex}}{i_{random}}$$

$$\beta^3 = \left( \frac{D_i}{D_{average}} \right)^3$$

Where  $i_{rex}$  and  $i_{random}$  are the respective number fraction of ‘*i*’ grains in the recrystallized material and in a random texture and  $D_i$  and  $D_{average}$  are the mean grain sizes of *i* and average

grains. If the grains are assumed to be spherical in size then the advantage factor is taken as  $\beta^3$  [51]. It is obvious that the recrystallization texture will be strengthened when  $\alpha$  and/or  $\beta^3$  are larger than 1.

### 2.3.1 Recrystallization Textures in HCP Metals

Recrystallization texture in case of FCC and BCC materials has been well understood. But in case of HCP material it is not completely understood. It is very easy to find texture examples in cubic system for any combination of alloy and processing modes. Progress have been made in developing models for recrystallization texture development in cubic systems, such as the oriented nucleation mode, oriented growth mode, or a combination of both [52], however it is very difficult to predict the texture evolution even in cubic system. It is sometimes experiential that recrystallization texture components hold crystallographic relationships to the original deformation textures and it can be described by rotations about simple crystal directions. For example, the BCC metals often show nearly  $25^\circ$  rotations around  $\langle 110 \rangle$  directions and FCC metals  $30\text{--}40^\circ$  rotations around  $\langle 111 \rangle$  [53]. Similarly in case of HCP metals, rotations of around  $30^\circ$  around  $\langle 0\ 0\ 0\ 1 \rangle$  and around  $90^\circ$  around  $\langle 1\ 0\ -1\ 0 \rangle$  have been reported [54, 55]. For recrystallized HCP metals the basal pole figures are often similar to those of rolling textures. The main basal texture components can be explained by approximately  $30^\circ$  rotation about  $\langle 0\ 0\ 0\ 1 \rangle$  that makes orientation change between rolled and annealed texture. When HCP metal with  $c/a$  ratio more than 1.623 like Zn and Cd is cold rolled then major texture component obtained is  $\{1\ 1\ -2\ 3\} \langle 1\ 1\ -2\ 3 \rangle$  [56]. HCP material with  $c/a$  ratio equal to 1.623 like Mg and Co is cold rolled,  $\{0\ 0\ 0\ 1\} \langle 1\ 0\ -1\ 0 \rangle$  is the major texture component obtained [56]. Similarly when a HCP material with  $c/a$  ratio less than 1.623 like Ti and Zr cold rolled then texture component is  $\{1\ 1\ -2\ 2\} \langle 1\ 0\ -1\ 0 \rangle$  [56]. When AZ31 Mg alloy is when hot extruded at about a temperature  $570^\circ\text{K}$  then major texture component is  $\{0\ 0\ 0\ 1\}$  basal fibre with a weak  $\{1\ 0\ -1\ 0\}$  and  $\{1\ 1\ -2\ 0\}$  fibre [57]. These are some examples of evolution of texture in HCP material when different processing conditions are applied onto it. From the above examples, it might be concluded that HCP metals and alloys exhibit a wider variety of recrystallization textures. These textures are strongly related to the initial deformation textures, annealing temperature and compositions. On the other hand, the the  $c/a$  ratio very strongly affects the initial deformation textures.

## 2.4 Recrystallization Textures in CP Titanium

Titanium and its alloys are of today's interest due to their high specific strength, high fatigue strength for which they are suitable for wide industrial application like aerospace and biomedical industry. At room temperature, commercial pure titanium (CP Ti) is a hexagonal close-packed crystal with the low lattice structure symmetry level and a small number of slip systems, which in turn makes it easier to form a texture during processing or deformation [58-60]. The first research on commercial pure titanium was conducted by Zhu et al [61-63]. Bozzolo et al. calculated the texture development in CP Ti during grain growth after recrystallization [64]. Chun et al. studied the consequence of deformed twins on microstructural and texture growth in CP Ti during cold rolling in plants [65-69]. When CP Ti is deep drawn the basal plane fiber texture shows a strong  $\{h k i l\}$  parallel to the normal direction (ND) fiber texture including four types of normal direction fibres texture with orientations  $(-1\ 2\ -1\ 5)$ ,  $(0\ 0\ 0\ 2)$ ,  $(0\ 2\ -2\ 1)$  and  $(-1\ 2\ -1\ 2)$  [18]. A better deep drawing property of CP Ti obtained when  $\{-1\ 2\ -1\ 5\} <1\ 0\ -1\ 0>$  texture component in the material increases. The texture in case of CP Ti can be classified or divided into three groups: (i) pyramid texture  $(-1\ 0\ 1\ 3)[5\ -2\ -3\ 0]$  and  $(-2\ 0\ 2\ 1)[1\ 0\ -1\ 5]$ , basal plane texture  $(0001)[2\ -1\ -1\ 0]$  and stronger prism texture  $(1\ 1\ -2\ 0)[0\ 0\ 0\ 1]$ . After annealing the main recrystallization texture is  $(-1\ 0\ 1\ 3)[5\ -2\ -3\ 0]$ . After annealing the basal plane texture vanished and come into existence in other forms because of slipping modes. After annealing the recrystallization texture inherits the components of the cold rolled texture but at the same time some recrystallization texture is also formed. With increase in the annealing time the cold rolling texture component in the material decreases and recrystallization texture increases [58].

## 2.5 Accumulative Roll Bonding (ARB)

In the present study ARB processing of cp-titanium was carried out before annealing. This was performed to achieve ultrafine grains. Materials with ultrafine grains have been produced by several unusual techniques such as rapid solidification, vapor deposition, mechanical alloying, cryogenic metal forming and intense plastic straining [70]. Exceptional processes such as cyclic extrusion compression (CEC) [71], torsion straining under high pressure (TS) [72], equal channel angular press (ECAP) [73] have already been applied to produce super metals. Accumulative roll bonding (ARB) is a relatively new method of severe plastic deformation proposed by Saito et al [74]. In this process the interfaces of the two strips to be

placed one over the other are cleaned properly by degreasing and wire brushing to remove the dirt. These interfaces are cleaned properly to achieve good bond strength. Then the two strips are placed over one another and joined together as in case of in a conventional roll bonding process. Then the rolled length is cut into two halves, cleaned properly, stacked together and rolled. This process is repeated again and again. So basically ARB is a process of cutting, stacking and rolling. Figure 2.6 shows a schematic of ARB processing [73]. ARB is carried out at elevated temperature but below the recrystallization temperature of the material due to the fact that above recrystallization temperature new strain free grains will form and the accumulated strain will cancel out. Low temperature results in insufficient ductility and bond strength. To attain sufficient bonding there exists a minimum reduction in thickness called as threshold deformation. If the homologous temperature is less than 0.5 then a sound joining can be achieved by a reduction greater than 50%. This signifies that material can be joined without recrystallization.

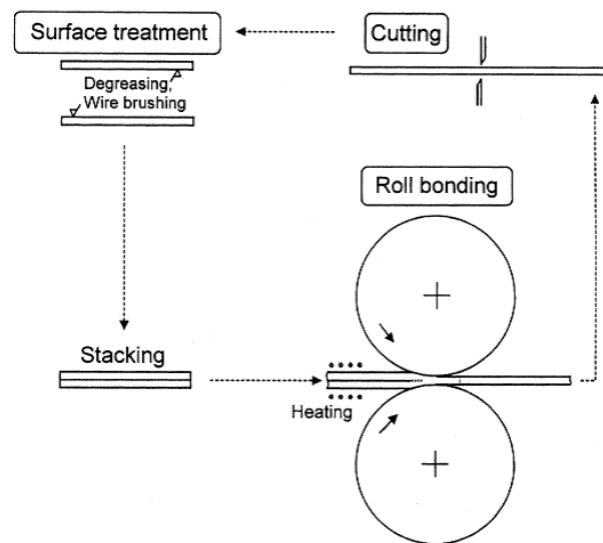


Figure 2.6. schematics of accumulative roll bonding. [74]

When the reduction per cycle is 50% with initial thickness  $t_0$ , then the final thickness of the sheet after  $n$  number of passes is:

$$t = \frac{t_0}{2^n}$$

Where 't' is the final thickness of the material.

Assuming Von Misses criterion, the equivalent plastic strain:

$$\epsilon = \left\{ \frac{2}{\sqrt{3}} \ln\left(\frac{1}{2}\right) \right\} \times n = 0.80n$$

Where 'n' is the total number of passes.

The process can introduce high plastic strain without any dimensional change of the specimen if the reduction in thickness per pass is limited to 50% because the increase in width is negligible in case of sheet rolling. The achieved strain is very high as by principle of this process we can go for any number of cycles. As this process is carried out below the recrystallization temperature it is a cold working process. ARB processing applies high strains as a result of which lamellar structural is produced in the work piece and also the low angle grain boundaries are converted to high angle grain boundaries which leads to the grain refinement [75]. When ARB is done on a sheet then texture evolution is seen in that sheet. There are two main conclusions drawn on the texture evolution in a ARB processed sheet: (a) the ARB processed sheet has less developed rolling texture due to the introduction of shear strain existing at the subsurface region into the inner part of the ARB processed sheet and (b) a complicated texture gradient develops during ARB depending upon the thickness location and microstructure [76].

### 3.1. Material and Sample Preparation

Commercial pure (CP) titanium (Grade-2) of chemical composition shown in table 3.1, was collected in the form of plates. From the plates, pieces of 80×40×5mm were cut. The pieces were rolled in a cold rolling mill and the thickness of the piece was reduced to 0.5mm with 5% reduction in each pass. Due to rolling the length of the piece increases. So after rolling the each piece was cut into 8-10 pieces (80×40×0.5mm) and were put in a furnace for annealing to enhance the ductility at 700°C with increase in temperature 4°C/min. After 2-3hrs the pieces were taken out from the furnace. Again each piece was cut into smaller pieces (80×10×0.5mm). Then from these smaller pieces two pieces were chosen for accumulative roll-bonding. One face of each piece was cleaned with wire brushing and then with acetone to remove the dirt. The two pieces were tied with the help of metallic wire with the cleaned surfaces one over the other. Now cold rolling is done on this and the two pieces tied turns into one piece with increase in length. Then the length of this ARB processed piece was measured and was cut into equal two halves. Again one face from each were cleaned with wire brushing and then with acetone, tied with the help of metallic wire with cleaned faces one over the other and cold rolling is done. Six passes were taken and in every pass the same process was repeated. In every pass the reduction in thickness is limited to 50%. So after each pass the thickness of the new sample obtained is 0.5mm only. After completion of six passes the final sample piece for the texture study was prepared. From the prepared sample small pieces were cut for annealing. The isochronal annealing was done at different temperatures (200°C, 300°C, 400°C, 500°C and 600°C) in an inert atmosphere for 1 hour. Subsequently annealing was carried out at 600°C for 5sec, 10sec, 20sec, 30sec, 90sec, 120sec, 300sec, 600sec, 1200sec, 1800sec and 3600sec. The annealed samples were electro-polished using an electrolyte of methanol and perchloric acid (90:10) at 21V before different characterizations.



## 3.2 Characterization Techniques

### 3.2.1 X-Ray Diffraction (XRD)

XRD was carried out at IIT Bombay in a Panalytical MRD system. Five different pole figures, (01-11), (01-12), (01-13) & (11-24), were measured and subsequent ODF was estimated using a commercial software Labo Tex 3.0 [77]. Table 3.1 Chemical composition (in wt.%) of CP titanium used in the present study.

Fe	C	N	H	O	Ti
0.034	0.004	0.004	0.0004	0.134	Balance

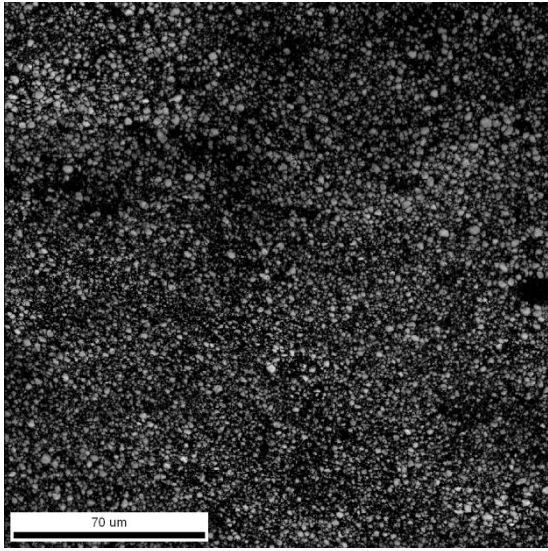
### 3.2.2 Electron Backscattered Diffraction (EBSD)

EBSD was carried out in a Fei-quanta SEM (scanning electron microscope) at IIT Bombay. EBSD of selected samples (mostly samples annealed for longer time) were measured. It was difficult to generate the kikuchi patterns in the samples annealed for smaller times.

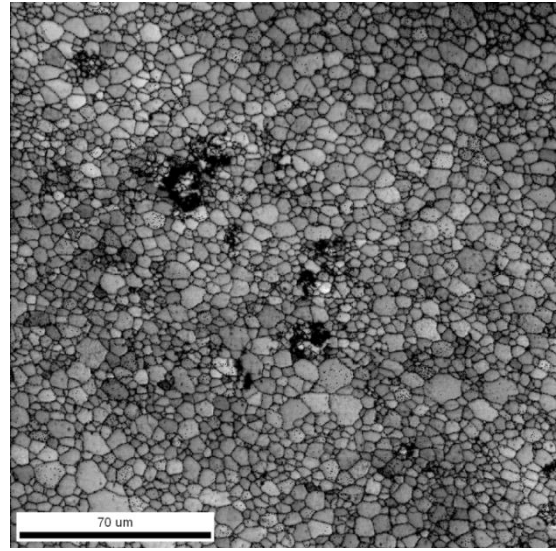
### 4.1 Results

Figure 4.1 shows the image quality maps of isochronal annealed CP-Titanium samples. The figure shows only 500°C and 600°C annealed samples. It may be noted that EBSD measurement of other isochronal annealed samples i.e. 200, 300 and 400°C, were difficult because of difficulty in obtaining kikuchi diffraction patterns. The samples were not properly annealed and diffused kikuchi diffraction patterns were obtained, indexing of such patterns was difficult. Figure 4.2 shows inverse pole figure maps of 500 and 600°C annealed cp-titanium samples. This shows a better quality of microstructure compared to figure 4.1. The black regions in the micrographs have confidence index less than 0.1. Very low confidence index ( $<0.1$ ) points were uncertain points in the microstructure. In the subsequent EBSD analysis all such points (i.e. confidence index  $<0.1$ ) were filtered. These two figures visually show that the cp-titanium sample was fully recrystallized at 600°C.

Figure 4.3 shows that the image quality maps of cp-titanium sample annealed at 600°C for 300sec, 600sec, 1200sec, 1800sec and 3600sec. This clearly shows that the percentage of recrystallization gradually increases with time. From such images, the percentage of recrystallization was calculated and is shown in figure 4.4. For such calculation, the grains greater than 2microns and the grain orientation spread less than 0.76 was considered. Grain orientation spread is the misorientation between all measurement points of the grain and grain average orientation. For a fully recrystallized grain it should be zero but grain orientation spread of 0.76 is the instrument tolerance. The percentage recrystallization increases with increase in annealing time.

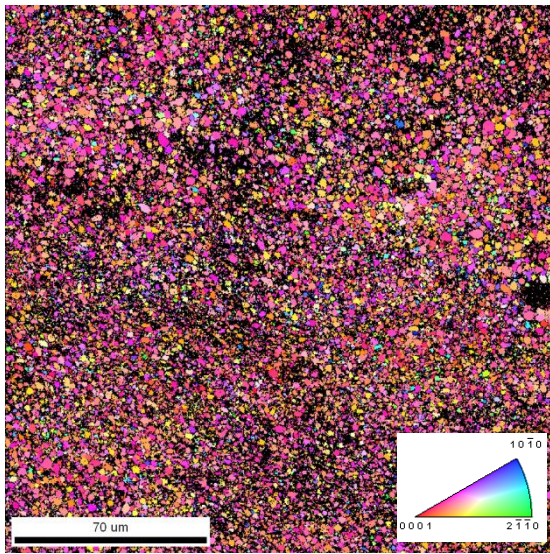


(a)

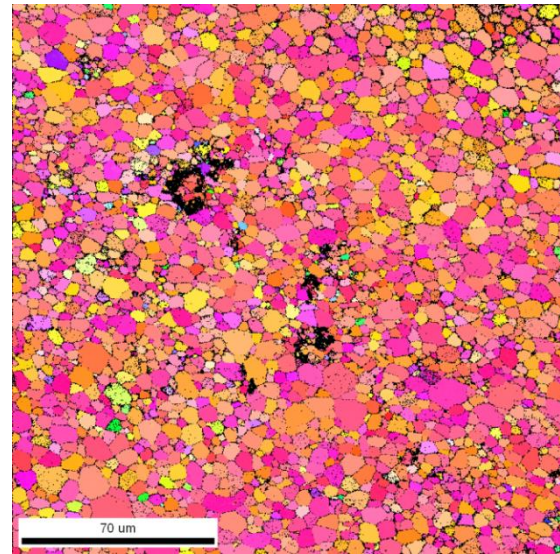


(b)

Figure 4.1. Image quality (IQ) maps of isochronal annealing (for 1hr) of cp-titanium samples at 500°C (a) and 600°C (b).



(a)



(b)

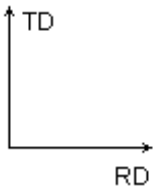


Figure 4.2. Inverse pole figure (IPF) maps of isochronal annealing (for 1hr) of cp-titanium samples at 500°C (a) and 600°C (b).

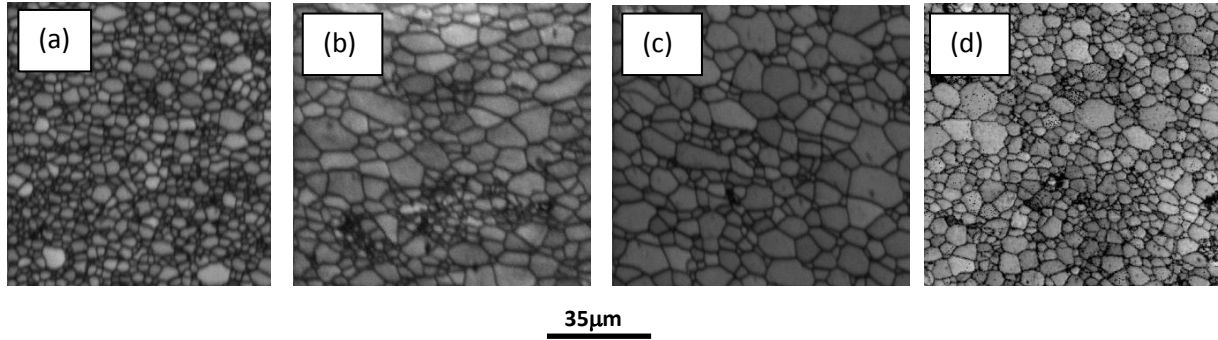


Figure 4.3. Image quality (IQ) maps of cp-titanium annealed at 600°C for; (a) 600sec, (b) 1200sec, (c) 1800sec, and (d) 3600sec.

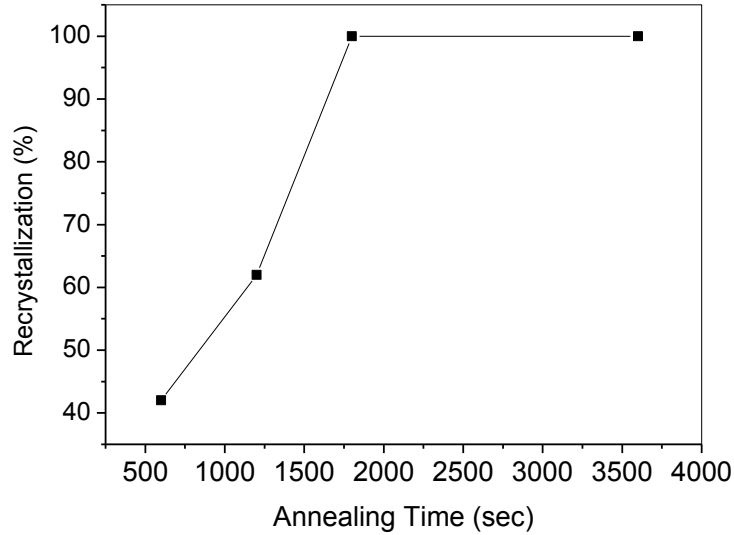


Figure 4.4. Percentage of recrystallization as a function of annealing time during annealing of cp-titanium at 600°C.

Figure 4.5 shows the XRD plot of cp-titanium samples annealed at 600°C for different soaking times. From a dominant peak intensity of (10-11) plane, development of peak intensities of (10-12), (10-13) and (11-24) planes was observed. This qualitatively confirms a development of texture in the samples. The texture development during annealing of the samples was represented by pole figure (table 4.1) and orientation distribution function (figure 4.6, and table 4.2). From the plots of pole figure it may be observed that the pole intensities of (10-12), (10-13) and (11-24) increases with increase in annealing time. Also these poles were rotated exactly in the rolling direction from a deviation of  $\sim 26^\circ$  of the rolling direction.



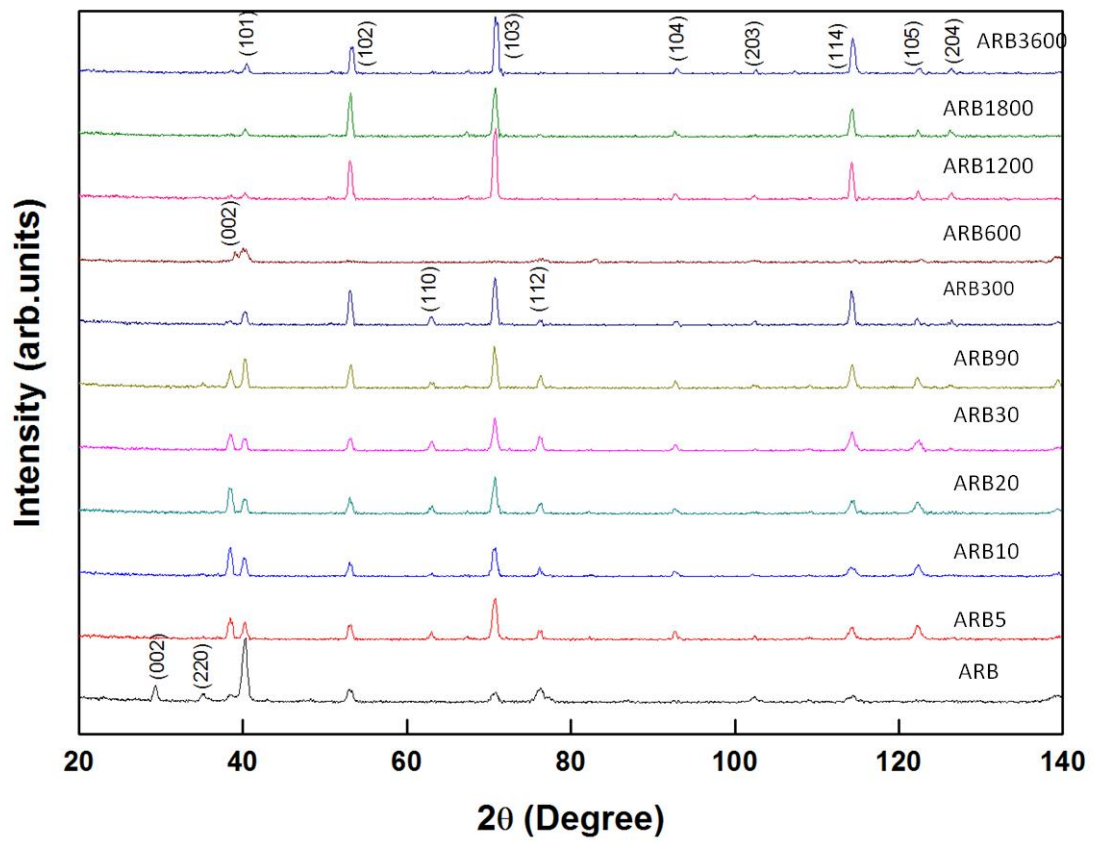
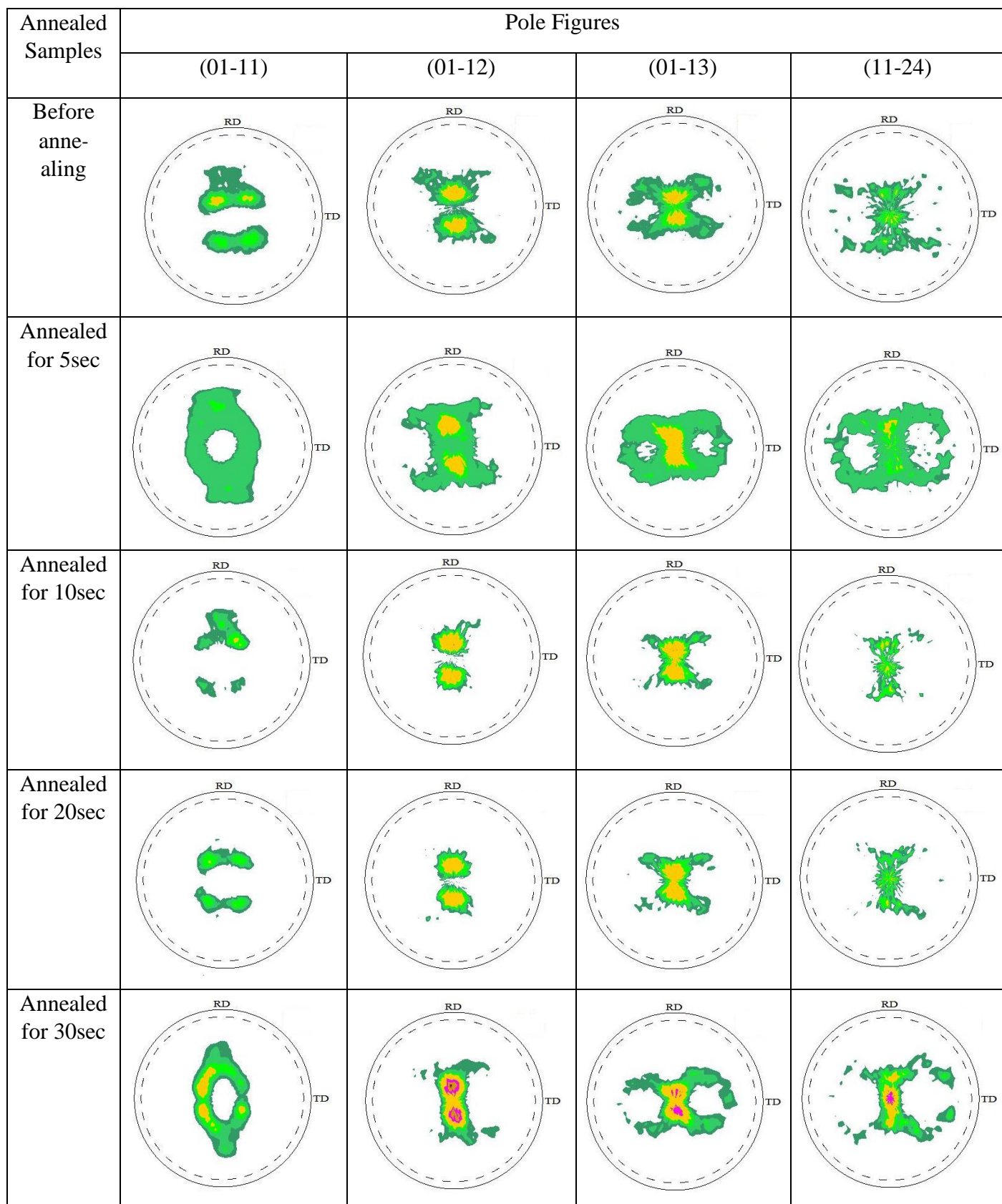
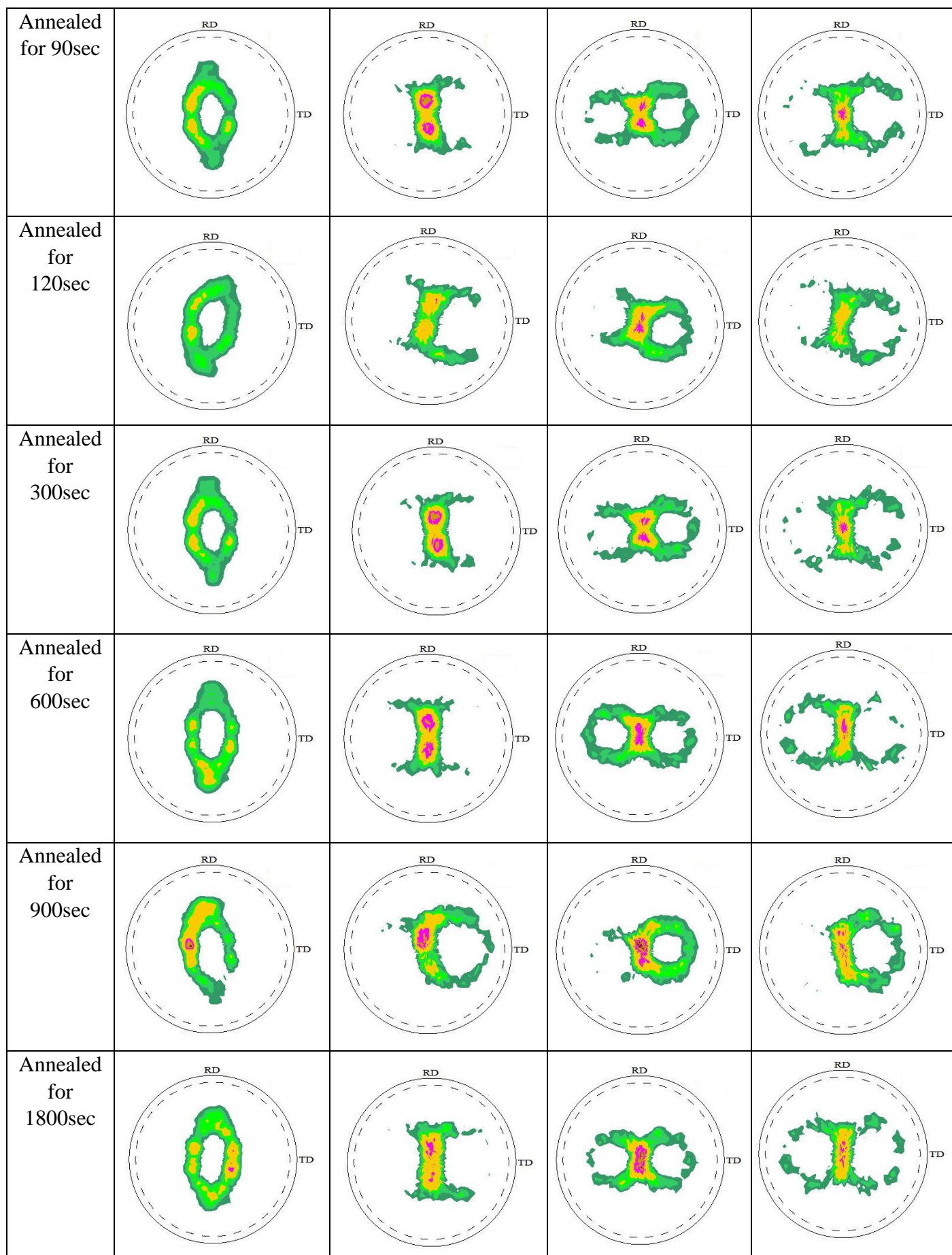
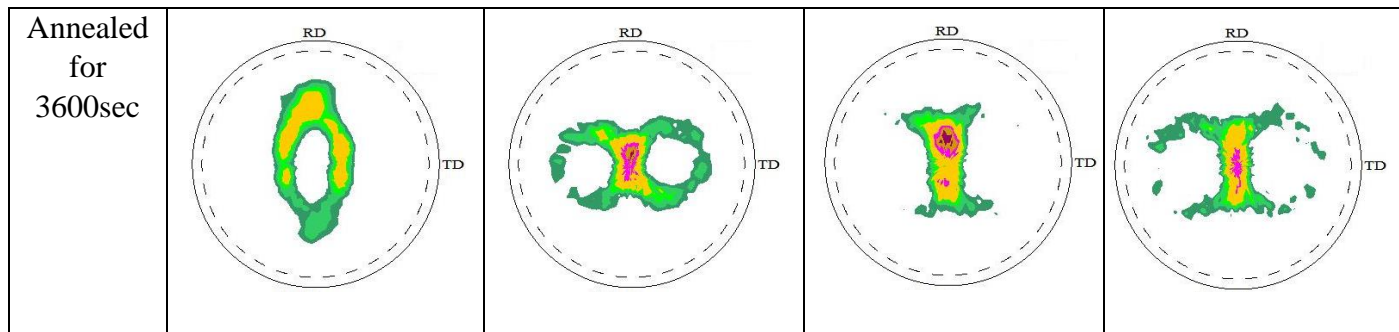


Figure 4.5. XRD plot of cp-titanium samples annealed at 600°C for different soaking time.

Table 4.1. Pole figures of different annealed cp-titanium samples. The contour levels are at 1.5, 2, 2.5, 3, 5, 6 and 7 times random.

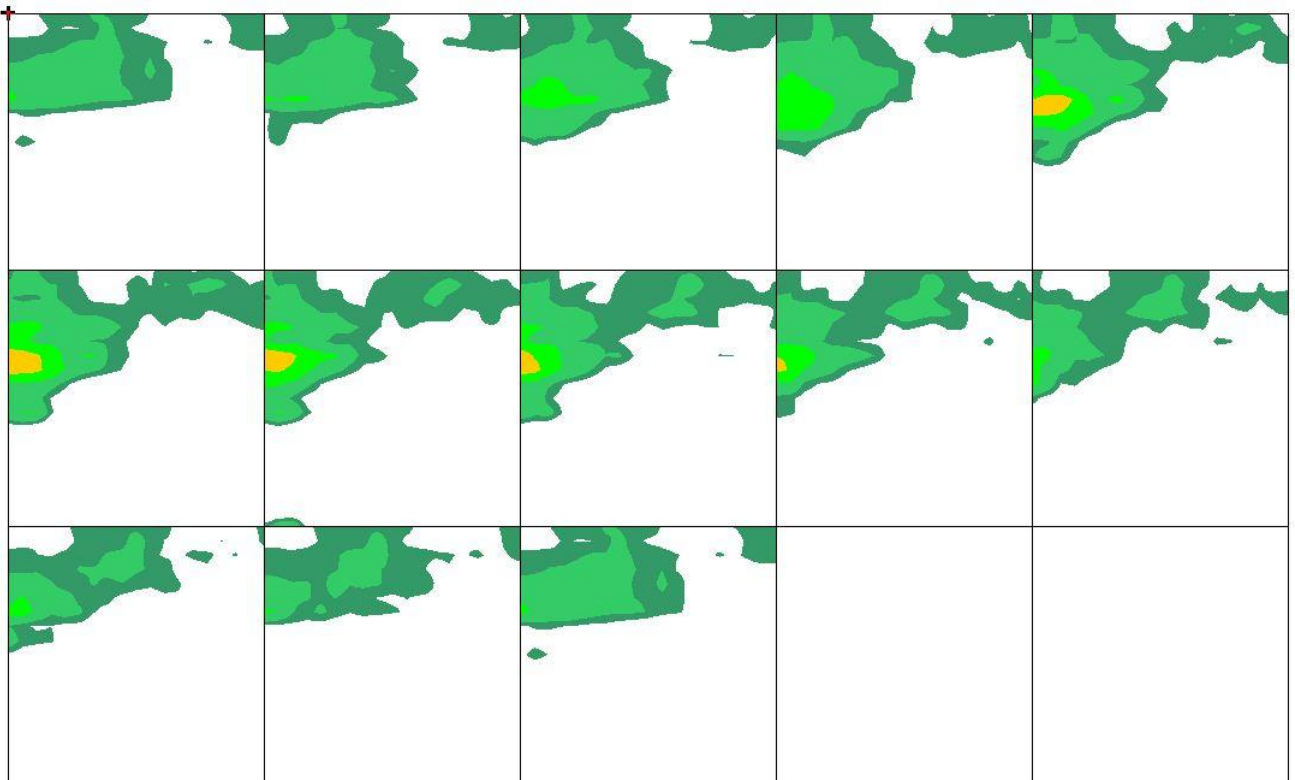






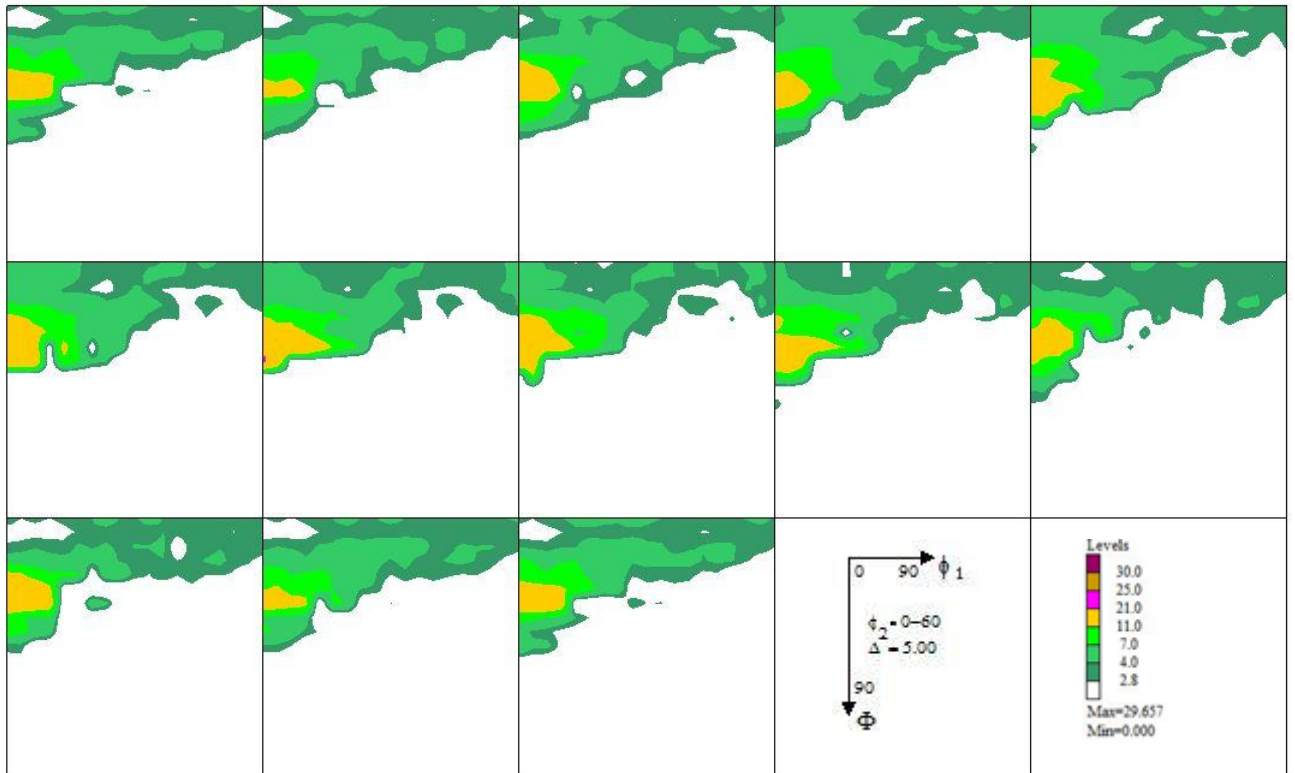
Following observations can be made from the ODF plots:

- The maximum odf intensity i.e.  $f(g)$  values increases with increase in annealing time (see figure 4.7)
- New orientations were developed with increasing annealing time (see figure 4.6 and table 4.2). Initially,  $(1\ 1\ -2\ 4)[3\ 1\ -4\ -1]$  orientation was dominant in the sample before annealing. Whereas with increase in annealing time,  $(0\ 0\ 0\ 1)[1\ -3\ 2\ 0]$  orientation was developed. Also at highest annealing time,  $(1\ 1\ -2\ 4)[6\ -2\ -4\ -1]$  orientation, i.e. the initial orientation, was developed.

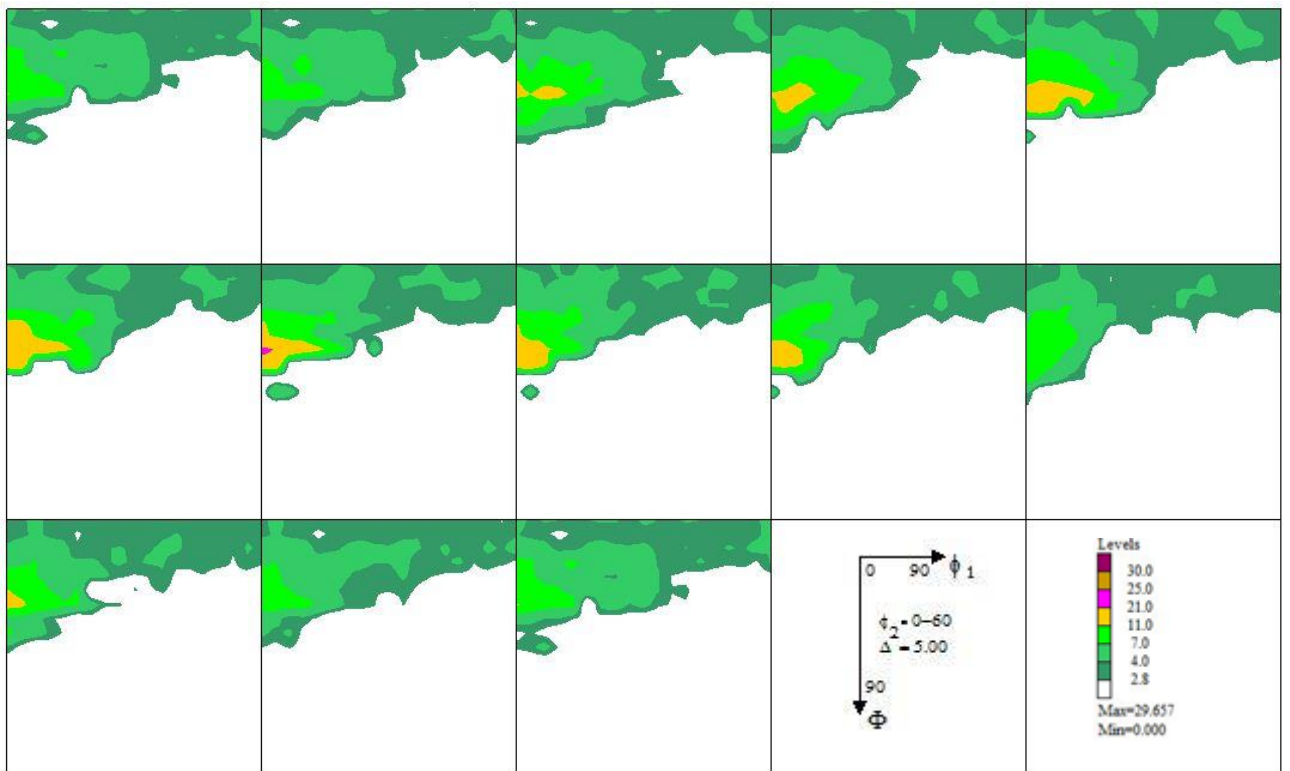


(Before annealing)

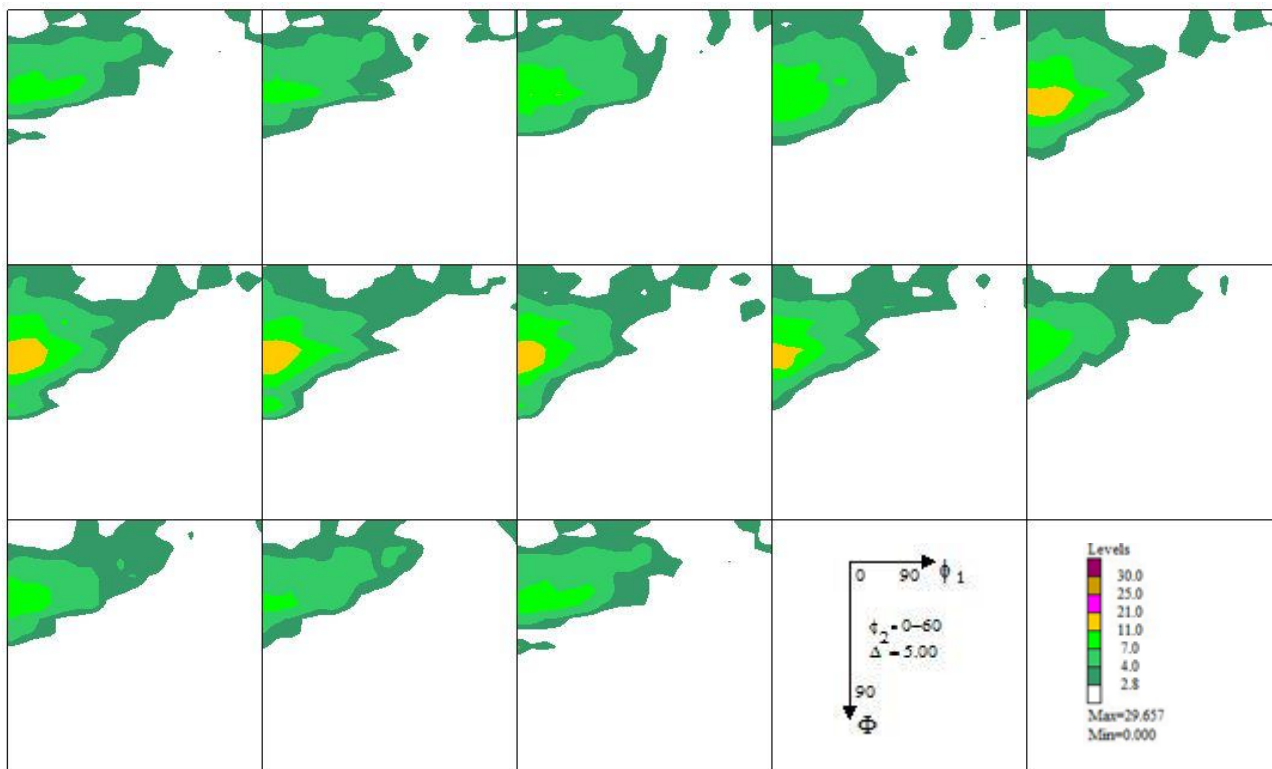




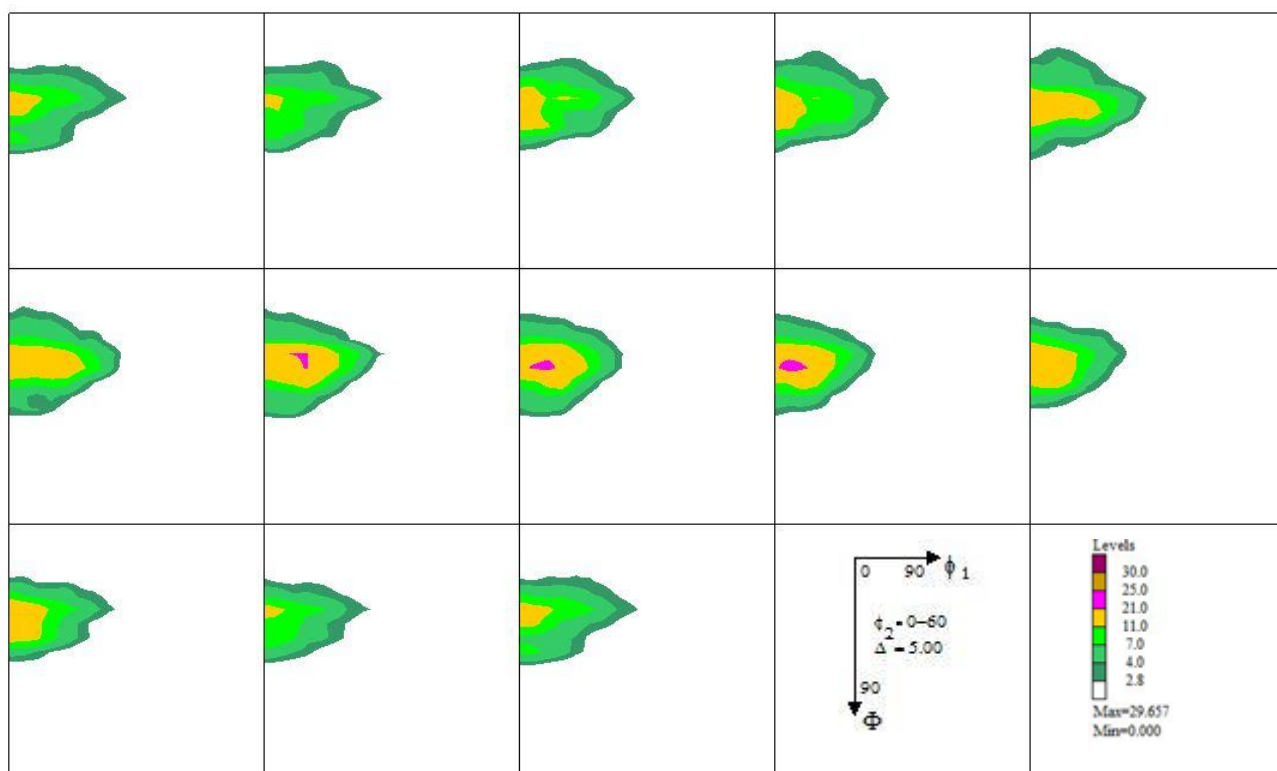
(Annealing for 5sec)



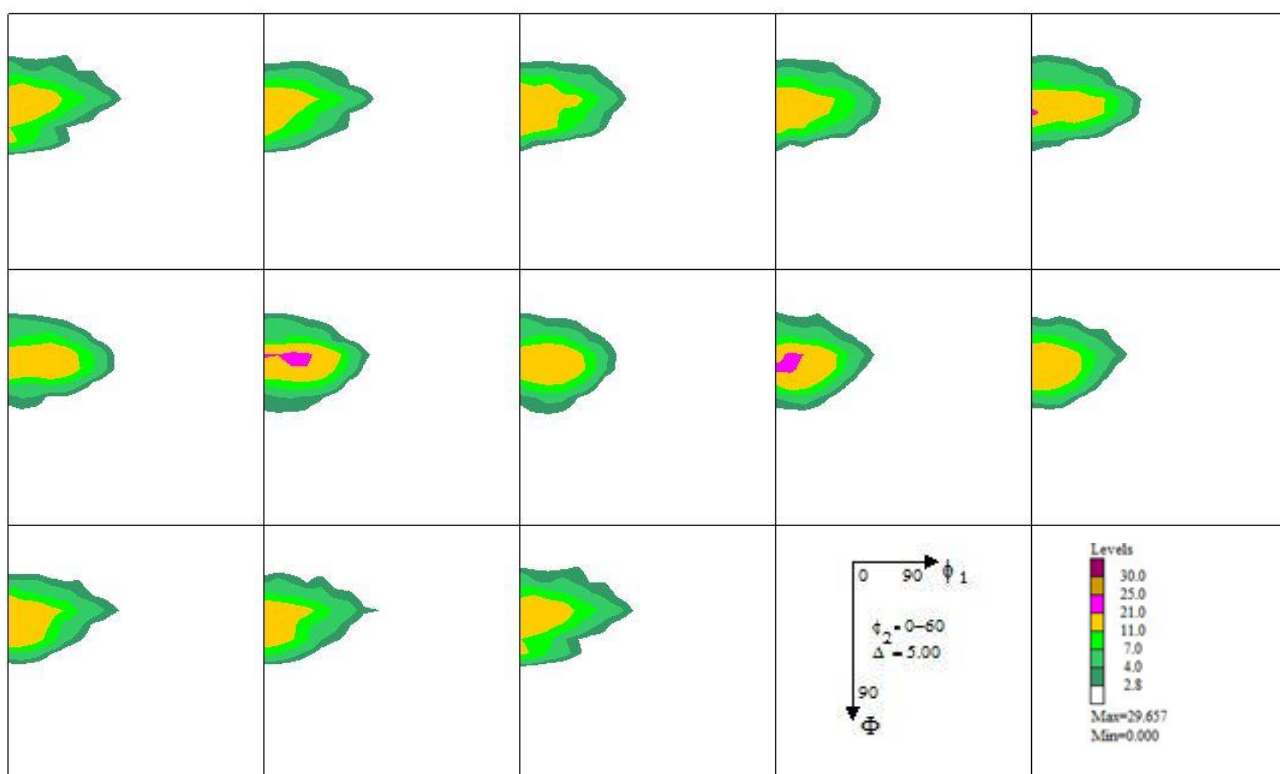
(Annealing for 10sec)



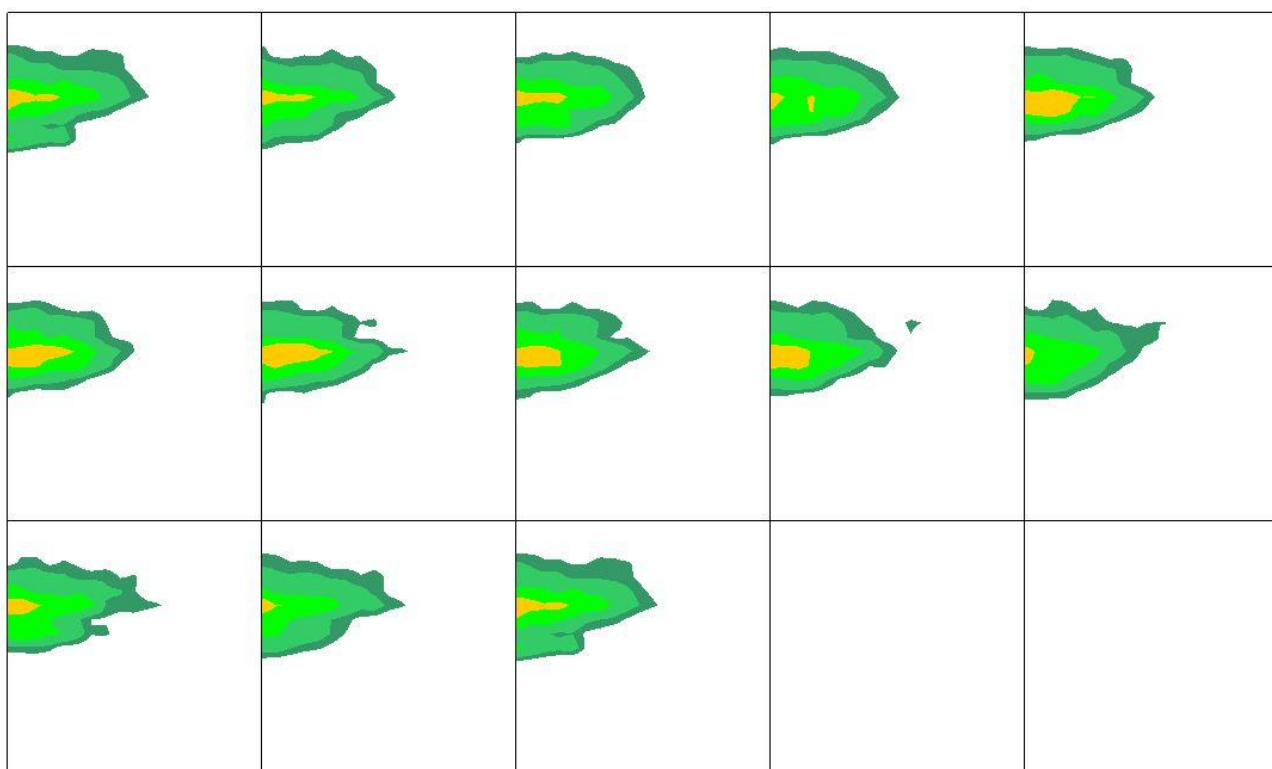
(Annealing for 20sec)



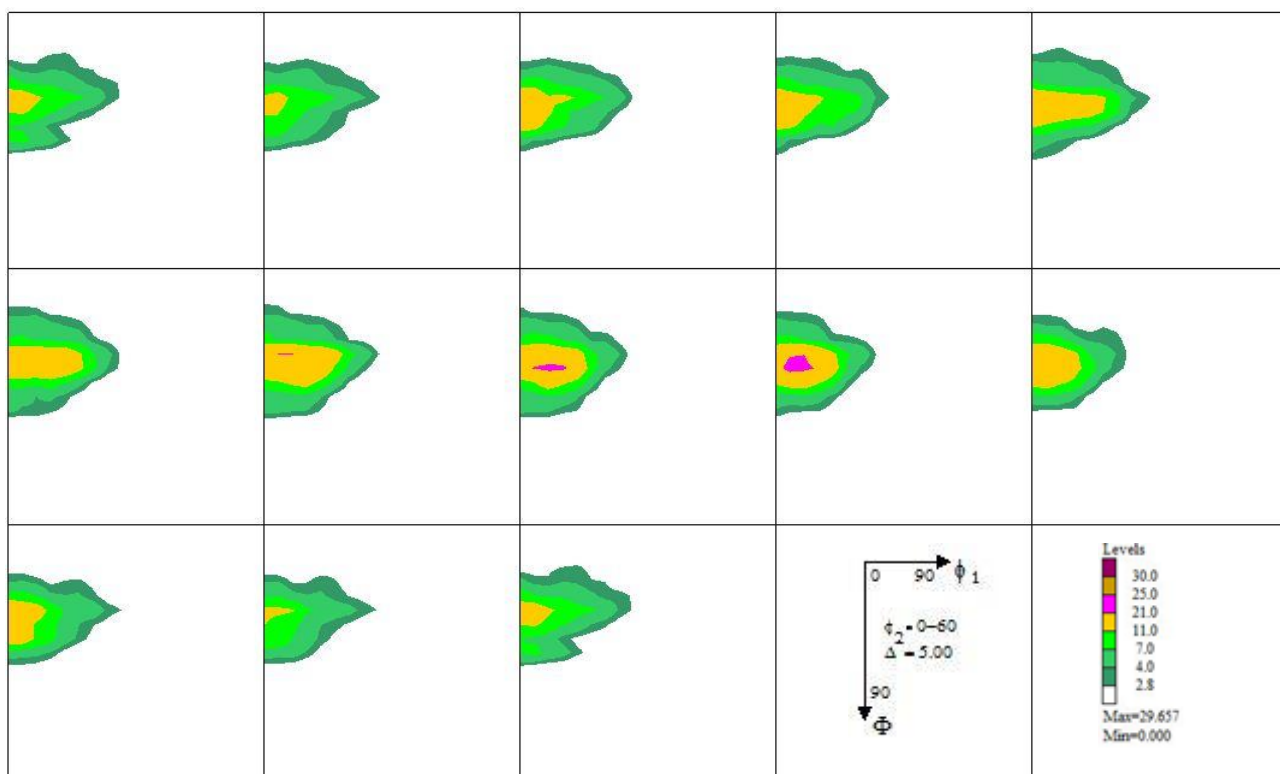
(Annealing for 30sec)



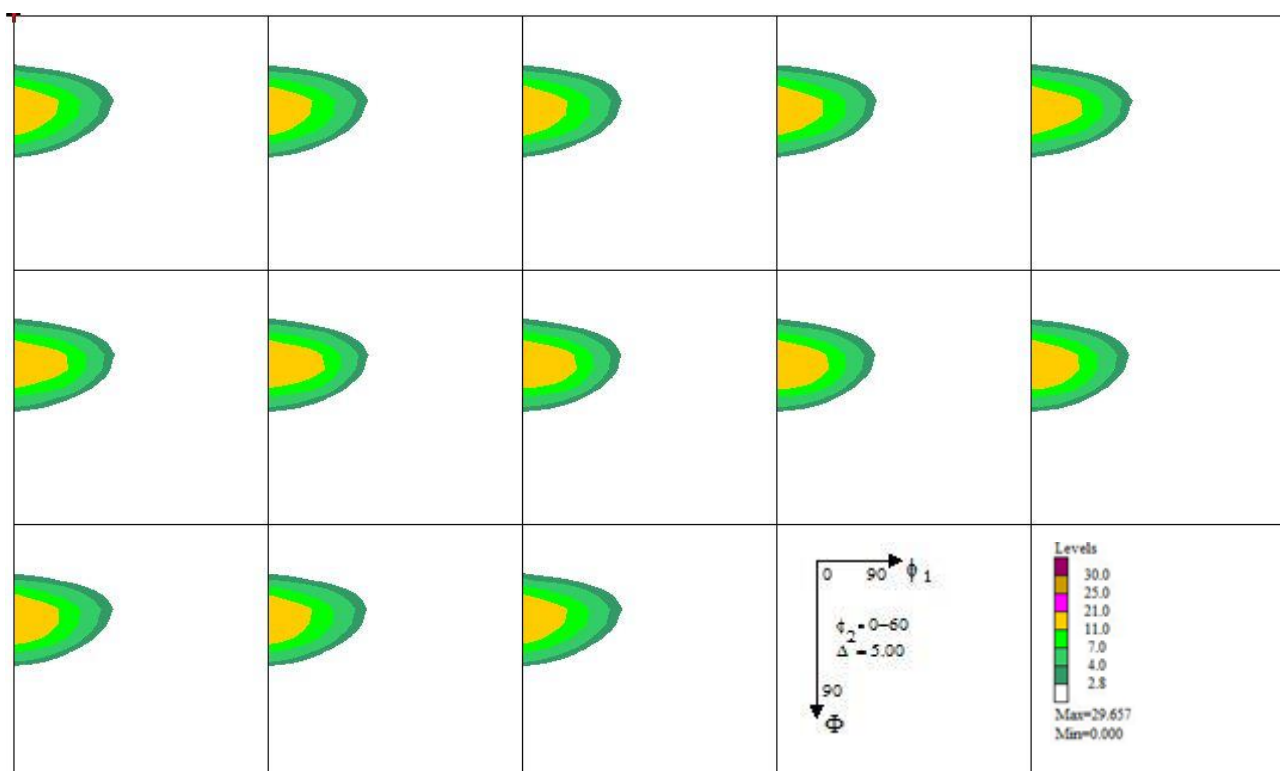
(Annealing for 90sec)



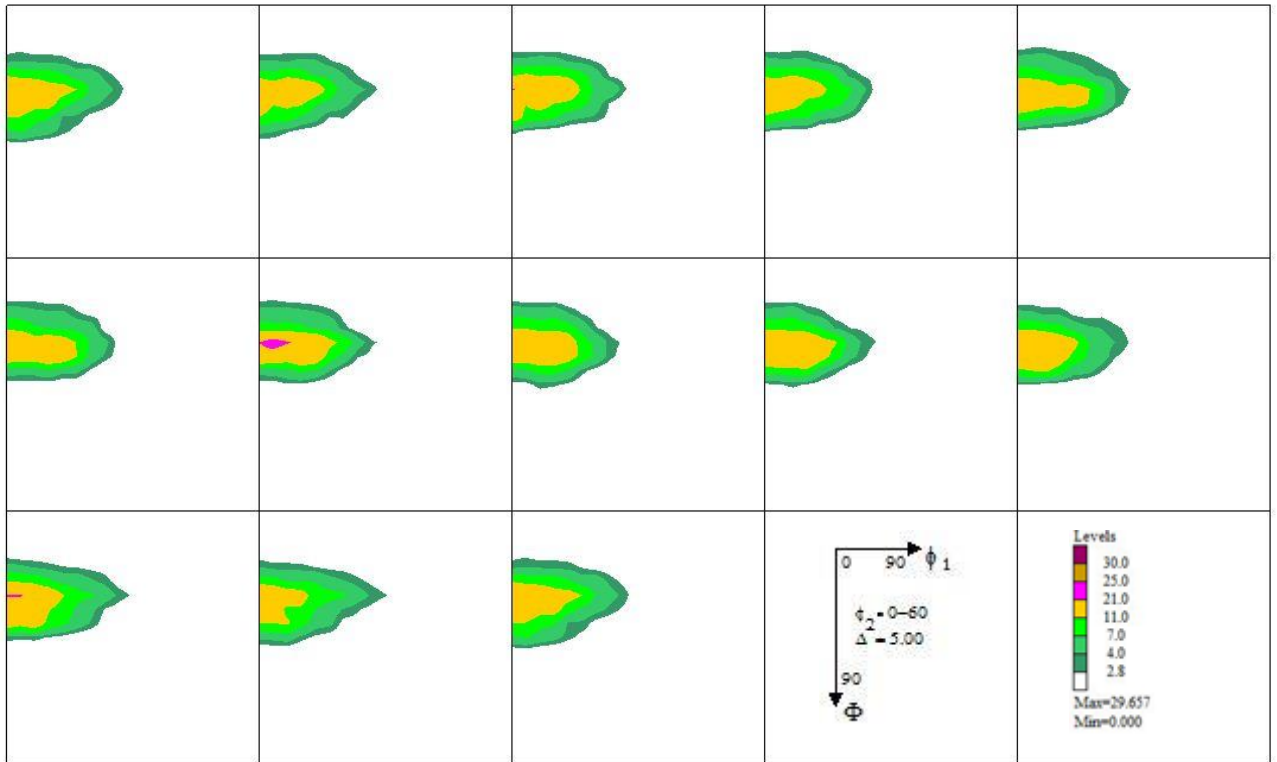
(Annealing for 120sec)



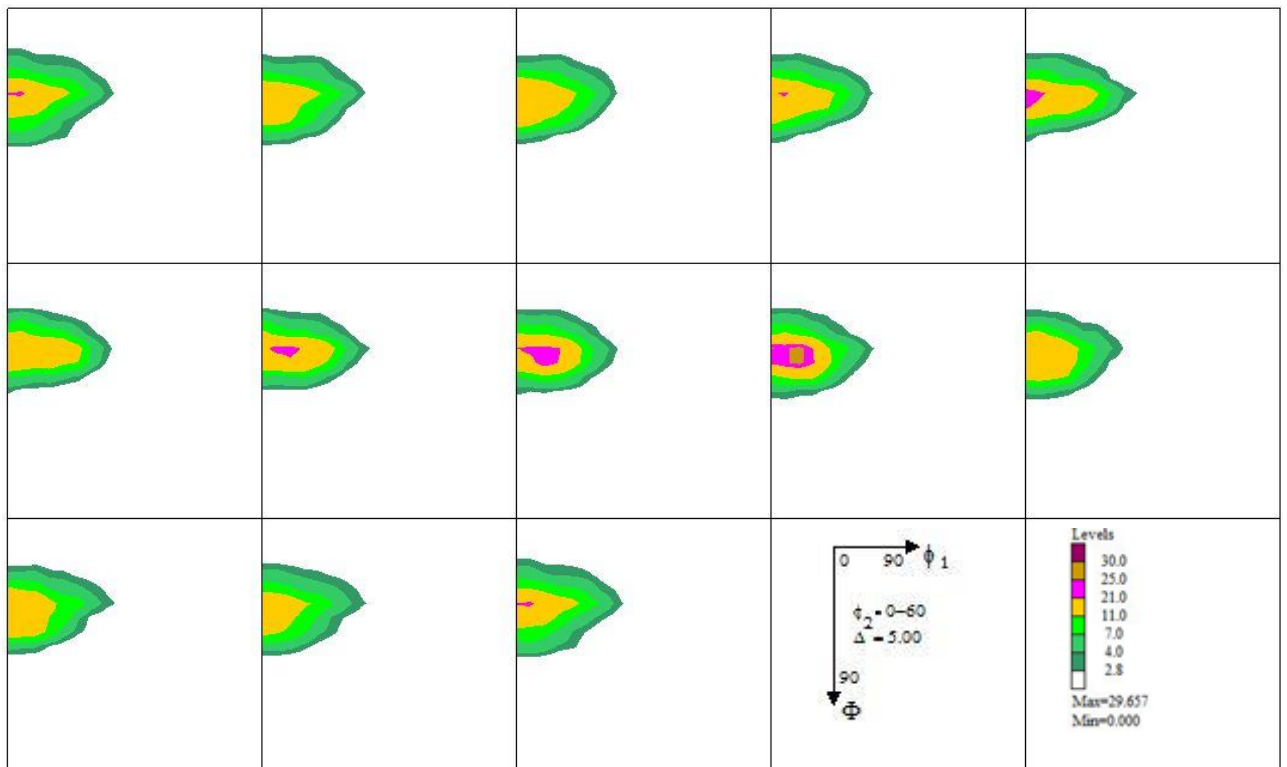
(Annealing for 300sec)



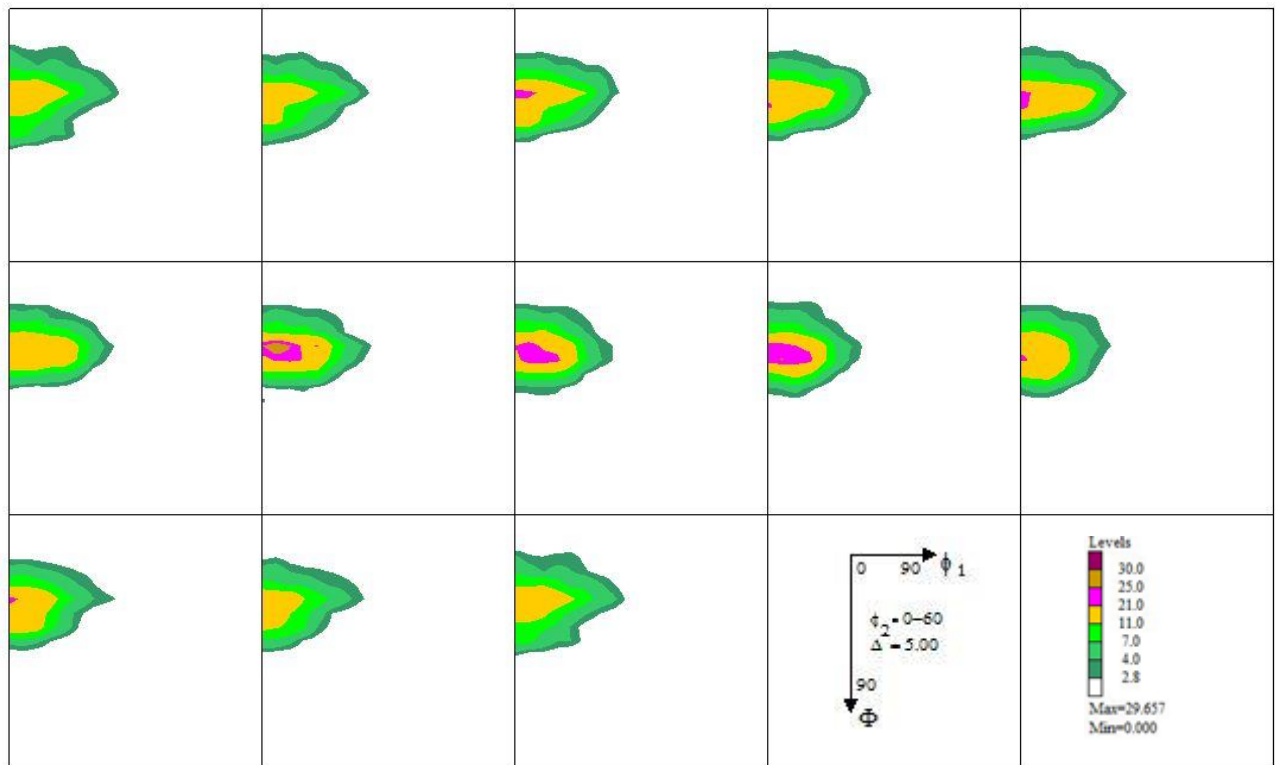
(Annealing for 600sec)



(Annealing for 1200sec)



(Annealing for 1800sec)



(Annealing for 3600sec)

Figure 4.6. ODF plots, at constant  $\phi_2$ , of different annealed CP-Titanium samples. The contour levels are similar in all the plots.

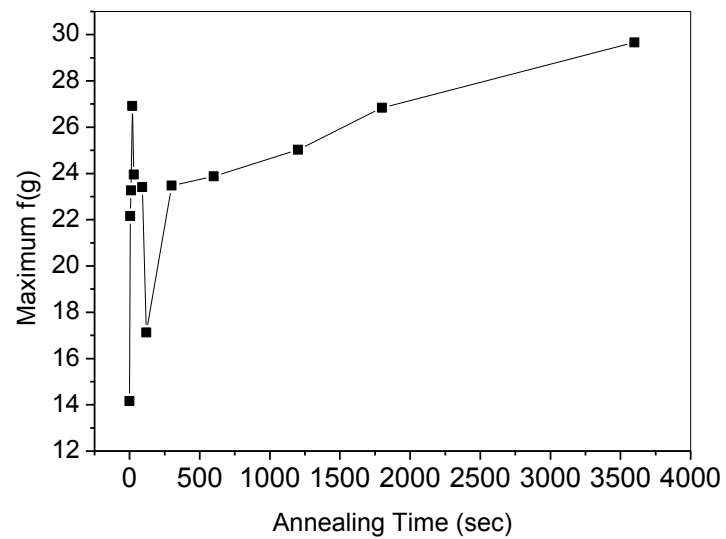


Figure 4.7. Maximum ODF intensity (maximum  $f(g)$ ) values as a function of annealing time for the annealed CP-Titanium samples.

Table. 4.2. Important texture developments during annealing of cp-titanium.

Annealed Samples	ORIENTATION	
	$\varphi_1, \Phi, \varphi_2$	(h k i l)[u v t w]
Before Annealing	0 30 30	(1 1 -2 4)[3 1 -2 -1]
Annealed for 5sec	5 30 30	(1 1 -2 4)[5 -1 -4 -1]
Annealed for 10sec	0 30 30	(1 1 -2 4)[3 1 -2 -1]
Annealed for 20sec	0 30 30	(1 1 -2 4)[5 -1 -4 -1]
Annealed for 30sec	5 35 40	(2 1 -3 7)[1 -2 1 0]
Annealed for 90sec	10 35 35	(0 0 0 1)[4 -9 5 0]
	10 35 35	(1 1 -2 4)[5 -9 4 1]
Annealed for 120sec	10 30 30	(1 1 -2 1)[4 3 -1 -1]
Annealed for 300sec	5 35 40	(0 0 0 1)[1 -3 2 0]
	5 35 40	(2 1 -3 7)[1 -2 1 0]
Annealed for 600sec	0 35 40	(2 1 -3 7)[1 -2 1 0]
Annealed for 1200sec	0 30 30	(1 1 -2 4)[3 1 -2 -1]
Annealed for 1800sec	10 35 35	(1 1 -2 4)[6 -10 4 1]
	5 30 40	(0 0 0 1)[1 -3 2 0]
	5 35 40	(3 1 -4 6)[3 -15 12 1]
Annealed for 3600sec	0 30 30	(1 1 -2 4)[6 -2 4 -1]



## 4.2 Discussions

As per reported literature, recrystallization texture of a material is dependent on cold rolling, starting texture and microstructure, chemical composition and amount of grain growth overlapping with recrystallization [6,41,42]. In the present study the dominant orientation was (11-24)  $\langle 31-4-1 \rangle$ , starting from ARB processing to annealing at highest time. However, during intermediate annealing (0001) [1-320] orientation was developed. The strength of (11-24)  $\langle 31-4-1 \rangle$  orientation was increased with increase in annealing time. It has been reported that with a similar starting texture, achieved by conventional rolling of cp-titanium, produced basal, (0001)  $\langle 1-100 \rangle$ , orientation and non-basal, (21-37)  $\langle 1-2-10 \rangle$ , (3 1 -4 9)  $\langle 2 -15 13 1 \rangle$  and (5 1 -6 15)  $\langle 1-540 \rangle$ , orientations with increased annealing time [78]. The strong texture development during annealing of ARB processed samples may be attributed due to larger strain in the samples.



### 5.1 Conclusions

- Recrystallization texture increases with increase in annealing time.
- The initial texture i.e.  $(1\ 1\ -2\ 4)[3\ 1\ -4\ -1]$  orientation was strengthened with increasing annealing time.  $(0\ 0\ 0\ 1)[1\ -3\ 2\ 0]$  orientation was developed during intermediate annealing time.

### 5.2 Scope for Further Study:

Recrystallization texture in a two-phase titanium alloy may be an interesting subject of interest. As observed in the present study, the initial texture is only strengthened while annealing a cp-titanium. These results may be different in a two-phase alloy. Also the texture development in other hexagonal metals may be an interesting subject to investigate.

## References

1. D.H. Avery, W.F. Hosford, W.A. Backofen Trans. AIME, 233 (1965), p. 71.
2. E.W. Kelley, W.F. Hosford. Trans. AIME, 242 (1968), p. 654.
3. Jay Chakraborty, Kishor Kumar, R. Ranjan, Sandip Ghosh Chowdhury, S.R. Singh Solid State Phenomena Volume 160(2010) pp109-116.
4. W. Mao, JMEPEG (1999) 8:556-560.
5. W. Köster, Beobachtungen an Kupfer zum Gesetzmäßigen Gefügebau nach der Rekristallisation, *Z. Metallkunde*, Vol 18, 1926, p 112-116 (in German)
6. H. Hu, Recovery, Recrystallization and Grain Growth, *Metallurgical Treatises*, J.K. Tien and J.F. Elliott, Ed., Metallurgical Society of AIME, 1981, p 385-407
7. W. Mao, J. Hirsch, and K. Lücke, Influence of the Cube Starting Texture on Rolling and Recrystallization Texture Development, Proceedings of 8th International Conference of Textures of Materials.
8. J.S. Kallend and G. Gottstein, Ed., The Metallurgical Society Inc., Pennsylvania, 1988, p 613-618.
9. A.D. Rollett, P. Kalu, D. Waryoba, 27-750, Spring 2006.
10. E.A. Calnan and C.J.B. Clews Philosophical Magazine Series 7 Volume 42, Issue 329, 1951.
11. Roger D. Doherty, Progress in Materials Science Vol. 42. pp 39-58. 1997.
12. K T Kashyap, Bull. Mater. Sci., Vol. 24, No. 1, February 2001, pp. 23–26. © Indian Academy of Sciences.
13. Verlinden, Driver, Samajdar and Doherty, Thermo-Mechanical Processing of Metallic Materials, 1st Edition. Volume 11.
14. K. Yoshimi, S. Ishiyama, S. Hanada, Y. Murayama, *physica status solidi (a)* **Volume 124**, issue pages 81–94, 16 March 1991.
15. H.-R. Wenk, I. Lonardelli, D. Williams, **Volume 52, Issue 7**, 19 April 2004, Pages 1899–1907.
16. Delannay L., Logé R.E., Signorelli J.W., Chastel Y., Evaluation of a multisite model for prediction of rolling textures in hcp metals, *Int. J. of Form. Proc.* vol. 8 2005, p.131.

17. Satyam Suwas and Nilesh P. Gurao, Journal of the Indian Institute of Science VOL 88:2 Apr–Jun 2008 journal.library.iisc.ernet.in.
18. Y.N. Wang and J.C. Huang, Materials Chemistry and Physics 81 (2003) 11–26.
19. Heatherly M. and Hutchinson W. B., An Introduction to Texture in Metals, Monograph no.5, The Institution of Metallurgist London 197.
20. Vinayak Deshmukh, Utpal Singha, Sunil Tonpe and N. Saibaba, Transactions of The Indian Institute of Metals, vol 63,issue 2-3, April-June 2010, pp 397-402.
21. F. Roters, P. Eisenlohr, L. Hantcherli, D.D. Tjahjanto, T.R. Bieler, D. Raabe Acta Materialia 58 (2010) 1152–1211.
22. U.F. Kocks, C.N. Tome and H.R. Wenk, Texture and Anisotropy, pp. 181–202.
23. San-Yuan Chen, Materials Chemistry and Physics 45 (1996) 159–162.
24. S.L. Swartz, IEEE Trans. Electr. Insul., 25 (1990) 935–987.
25. L.H. Parker and A.F. Tasch, IEEE Trans. Circuits Devices, 6 (1990) 17–26.
26. J. E. Bailey and P. B. Hirsch, Proc. Roy. Soc. 267A, 11 (1962).
27. N. RAJMOHAN, J.A. SZPUNAR, and Y. HAYAKAWA, Textures and Microstructures, Vol. 32, pp. 153–174.
28. Sebastian Seippa, Martin F.-X. Wagner, Kristin Hockauf, Ines Schneider, Lothar W. Meyer and Matthias Hockauf, International Journal of Plasticity 35 (2012) 155–166.
29. Agnew, S.R., Horton, J.A., Lillo, T.M., Brown, D.W., 2004. Enhanced ductility in strongly textured magnesium produced by equal channel angular processing. Scripta Materialia 50, 377–381.
30. Barber, R.E., Dudo, T., Yasskin, P.B., Hartwig, K.T., 2004. Product yield for ECAE processing. Scripta Materialia 51, 373–377.
31. P.P. Bhattacharjee, R.K. Ray, A. Upadhyaya, Volume 488, Issues 1–2, 15 August 2008, Pages 84–91.
32. S. Barella, C. Mapelli and R. F. Riva, Revue de Métallurgie, Volume 107, Issue 7–8, July 2010, pp 275–291
33. Barrett C. S. and Massalski T. B., Structure of Metals, McGrawHill, New York, 1966.
34. T.R. McNelley, D.L. Swisher, M.T. Perez-Prado, Metall. Mater. Trans 33 (2002) 279.
35. O. Fischer, J. Schneider, Journal of Magnetism and Magnetic Materials 254 (2003) 302.

36. Bunge H. J., Z. Metallk. 56 (1965) 872.
37. Roe R.-J, Journal of Applied Physics 36, (1965) 2024.
38. A. Szpunar, in: H.J. Bunge (Ed.), Texture, Anisotropy in Magnetic Steels, Direction Properties of Materials, Cuvillier Verlag, Gttingen, (1988) 129.
39. Bessieres, J., Heizmann, J.J. and Eberhardt, A., Textures and Microstructures, (1991) 14,157.
40. Burgers WG, Louwerse PC. Über den Zusammenhang zwischen Deformationsvorgang und Rekristallisationstextur bei Aluminium. Zeitschrift für Physik 1931; 61 605-678.
41. Barrett CS. Recrystallization texture in aluminum after compression. Trans AIME 1940; 137 128-145.
42. Gottstein G. Evolution of recrystallization texture- classical approaches and recent advances. Materials Science Forum 2002; 408-412 1-24.
43. Humphreys F.J., Acta Mater., 45 (1997), 4231–4240.
44. Doherty R.D., Hughes D.A., Humphreys F.J., Jonas J.J., Juul Jensen D., Kassner M.E., King W.E., McNelley T.R., McQueen H.J. and Rollett A.D., Mater. Sci.Eng., A238 (1997), 219.
45. Dillamore I.L., Roberts J.G. and Bush A.C., Met. Sci., 13 (1979), 73.
46. Gil Sevillano J., Van Houtte P. and Aernoudt E., Prog. Mater. Sci., 25 (1980), 69–412.
47. Van Houtte P., Acta Metall. Mater., 43 (1995), 2859.
48. Samajdar I., Rabet L., Verlinden B. and Van Houtte P., ISIJ Intl., 3 (1998c), 539.
49. rsund R. and Nes E., Scripta Metall. Mater., 22 (1988), 671.
50. Berger A., Wilbrandt P.J., Ernst F., Klement U. and Haasen P., Prog. Mater. Sci., 32(1988), 1.
51. Doherty R.D., Scripta Metall., 19 (1985), 927.
52. O. Engler, Metall. Mater. Trans. 30A (1999) 1517.
53. H.J. Bunge, Texture Analysis in Materials Science, Butterworths Press, London, 1982.
54. F.J. Humphreys, P.N. Kalu, Textures Microstruct. 14–18 (1990) 703.
55. M. Hatherly, W.B. Hutchinson, An Introduction to Textures in Metals, Chameleon Press, London, 1990.

56. U.F. Kock, C.N. Tome, H.R.Wenk, *Texture and Anisotropy: Preferred Orientation in Polycrystals and Their Effect on Materials Properties*, Cambridge University Press, Cambridge, 1998.
57. M.T. Perez-Prodo, O.A. Ruano, *Scr. Mater.* 45 (2001) 89.
58. Hai-tao Jiang, Ji-xiong Liu, Zhen-li Mi, Ai-min Zhao, and Yan-jun Bi, *International Journal of Minerals, Metallurgy and Materials*, Volume 19, Number 6, June 2012, Page 530.
59. M.H. Yoo, Slip, twinning, and fracture in hexagonal close- packed metals, *Metall. Trans. A*, 12(1981), No.3, p.409.
60. M.J. Philippe, M. Serghat, P. Van Houtte, and C. Esling, Modelling of texture evolution for materials of hexagonal symmetry: II. Application to zirconium and titanium  $\alpha$  or near  $\alpha$  alloys, *Acta Metall. Mater.*, 43(1995), No.4, p.1619.
61. Z.S. Zhu, J.L. Gu, N.P. Chen, and Z.S. Yang, Research on the relationship between texture and mechanical property anisotropy in commercially pure titanium sheets, *Mater. Mech. Eng.*, 18(1994), No.2, p.23.
62. Z.S. Zhu, J.L. Gu, and N.P. Chen, The influence of cold rolling on the formation of recrystallization texture in titanium sheet, *Mater. Sci. Technol.*, 3(1995), No.2, p.49.
63. Z.S. Zhu, M.G. Yan, J.L. Gu, and N.P. Chen, Investigation of phase transformation textures and their influence factors in titanium sheet, *J. Aeronaut. Mater.*, 16(1996), No.1, p.19.
64. N. Bozzolo, N. Dewobroto, T. Grosdidier, and F. Wagner, Texture evolution during grain growth in recrystallized commercially pure titanium, *Mater. Sci. Eng. A*, 397(2005), No.1-2, p.346.
65. Y.B. Chun, S.H. Yu, S.L. Semiatin, and S.K. Hwang, Effect of deformation twinning on microstructure and texture evolution during cold rolling of CP-titanium, *Mater. Sci. Eng. A*, 398(2005), No.1-2, p.209.
66. G. Proust, C.N. Tomé, and G.C. Kaschner, Modeling texture, twinning and hardening evolution during deformation of hexagonal materials, *Acta Mater.*, 55(2007), No.6, p.2137.
67. Y.N. Wang and J.C. Huang, Texture analysis in hexagonal materials, *Mater. Chem. Phys.*, 81(2003), No.1, p.11.

68. J.M. Liu, I.G. Chen, T.S. Chou, and S.S. Chou, On the deformation texture of square-shaped deep-drawing commercially pure Ti sheet, *Mater. Chem. Phys.*, 77(2003), No.3, p.765.
69. T. Ungár, M.G. Glavicic, L. Balogh, K. Nyilas, A.A. Salem, G. Ribárik, and S.L. Semiatin, The use of X-ray diffraction to determine slip and twinning activity in commercial-purity (CP) titanium, *Mater. Sci. Eng. A*, 493(2008), No.1-2, p.79.
70. J. Gottstein G. Evolution of recrystallization texture- classical approaches and recent advances. *Materials Science Forum* 2002; 408-412 1-24.
71. Richert, J. and Richert, M., *Aluminium*, 1986, 62, 604.
72. Horita, Z., Smith, D. J., Furukawa, M., Nemoto, M., Valiev, R. Z. and Langdon, T. G., *J. Mater. Res.*, 1996, 11, 1880.
73. Valiev, R. Z., Krasilnikov, N. A. and Tsenev, N. K., *Mater. Sci. Engng*, 1991, A137, 35.
74. Y. SAITO, H. UTSUNOMIYA, N. TSUJI and T. SAKAI, *Acta mater.* Vol. 47, No. 2, pp.579-583, 1999.
75. M. Karlík, P. Homola, M. Slámová, *Journal of Alloys and Compounds* 378 (2004) 322–325.
76. L. Jiang, M.T. Pe´rez-Prado, P.A. Gruber, E. Arzt, O.A. Ruano, M.E. Kassner, *Acta Materialia* 56 (2008) 1228–1242.
77. LaboSoft s.c., [www.labosoft.com](http://www.labosoft.com).
78. S.K. Sahoo and Sidharth Pal, *Recrystallization texture in CP-titanium*, B.Tech thesis, 2013.